1-1-2012

Intermittent Arc Fault Detection And Location For Aircraft Power Distribution System

Anil Yaramasu
Ryerson University

INTERMITTENT ARC FAULT DETECTION AND LOCATION FOR AIRCRAFT POWER DISTRIBUTION SYSTEM

by

ANIL YARAMASU

Bachelor of Technology, Electrical and Electronics Engineering, JNTUK, India, 2009

A thesis

presented to Ryerson University

in partial fulfillment of the requirements for the degree of

Master of Applied Science

in the Program of

Electrical and Computer Engineering

Toronto, Ontario, Canada, 2012

AUTHOR'S DECLARATION

I hereby declare that I am the sole author of this thesis. This is a true copy of the thesis, including any required final revisions, as accepted by my examiners.

I authorize Ryerson University to lend this thesis to other institutions or individuals for the purpose of scholarly research.

I further authorize Ryerson University to reproduce this thesis by photocopying or by other means, in total or in part, at the request of other institutions or individuals for the purpose of scholarly research.

I understand that my thesis may be made electronically available to the public.

BORROWER'S PAGE

Ryerson University requires the signatures of all persons using or photocopying this thesis. Please sign below, and give address and date.

Name	Address	Date	Signature

ABSTRACT

Intermittent Arc Fault Detection and Location for Aircraft Power Distribution System

© Anil Yaramasu, 2012

Master of Applied Science

in the program of

Electrical and Computer Engineering

Ryerson University

This thesis addresses a non-destructive diagnostic method for intermittent arc fault detection and location. Intermittent arc faults appear in aircraft power systems in unpredictable manners when the degraded wires are wet, vibrating against metal structures, or under mechanical stresses, etc. They could evolve into serious faults that may cause on-board fires, power interruptions, system damage and catastrophic incidents, and thus have raised much concern in recent years.

Recent trends in solid state power controllers (SSPCs) motivated the development of non-destructive diagnostic methods for health monitoring of aircraft wiring. In this thesis, the ABCD matrix (or transmission matrix) modeling method is introduced to derive normal and faulty load circuit models with better accuracy and reduced complexity compared to the conventional differential equation approach, and an intermittent arc fault detection method is proposed based on temporary deviations of load circuit model coefficients and wiring parameters. Furthermore, based on the faulty wiring model, a genetic algorithm (GA) is proposed to estimate the fault-related wiring parameters, such as intermittent arc location and average intermittent arc resistance. The proposed method can be applied to both the alternating current (AC) power distribution system (PDS) and direct current (DC) PDS. Simulations and experiments using a DC

power source have been conducted, and the results have demonstrated effectiveness of the proposed method by estimating the fault location with an accuracy of +/- 0.5 meters on 24.6 meters wire. Unlike the existing techniques which generally requires special devices, the proposed method only needs circuit voltage and current measurement at the source end as inputs, and is thus suitable for SSPC-based aircraft PDS.

ACKNOWLEDGMENTS

I would like to express my sincere gratitude to my main supervisor, Dr. Guangjun Liu, for his valuable suggestions, help, patience, and guidance during this work. My sincere gratitude also goes to my co-supervisor, Dr. Bin Wu, for his help, suggestions and wisdom. They provided much of the input that helped me to produce presentable and superior research work.

My special thanks to Dr. Yinni Cao for her discussions, comments and suggestions during this work. I am thankful to my colleagues and friends at the Laboratory for Electric Drive Applications and Research (LEDAR), and those at the Systems and Control Laboratory for their friendship and discussions. I wish to thank Ryerson University for an International Graduate Scholarship.

I am very thankful to my brother, Mr. Venkata Yaramasu, for his valuable suggestions, help and motivation. Countless thanks to my mother, uncle and other family members for their help, support, encouragement and patience.

TABLE OF CONTENTS

LIST OF FIGURES

LIST OF TABLES

LIST OF PUBLICATIONS

[1] A. Yaramasu, Y. Cao, G. Liu, and B. Wu, “Intermittent wiring fault detection and diagnosis for SSPC based aircraft power distribution system,” IEEE/ASME International Conference on Advanced Intelligent Mechatronics (AIM), pp. 1117-1122, July 11-14, 2012.

[2] A. Yaramasu, Y. Cao, G. Liu, and B. Wu, “Intermittent arc fault detection and location for SSPC based aircraft power distribution system,” first draft version submitted for IEEE Transactions on Aerospace and Electronic Systems, 2012.

NOMENCLATURE

I	current
V	voltage
r	resistance
l	inductance
c	capacitance
g	conductance
ρ	conductivity
a	cross-sectional area
d	wire length
d_1	distance of fault location from the SSPC
d_2	distance of fault location from the load end
Z_{L}	load impedance
z	wire series impedance
y	wire shunt admittance
R_{L}	load resistance
R_{arc}	arc resistance
I_{arc}	arc current
V_{arc}	arc voltage
$\hat{\theta}$	unknown model coefficient vector
N	number of frequency points
M	model vector
e	error value
δ	predetermined threshold value
K	predetermined fitness limit value
P_{c}	crossover probability
P_{m}	mutation probability

CHAPTER 1

INTRODUCTION

1.1 Overview

The power demands in modern aircrafts have been increasing with the concept of more electric aircraft (MEA), where the hydraulic, pneumatic, mechanical equipment in the domains of propulsion, control and auxiliary systems have been replaced with electrical systems [1]. In the meantime, the wiring related problems are also rising, with the prevalence of MEA, aging of aircraft wiring, augmented customer power demands, and the high voltage aircraft power distribution systems (PDS) which aims to reduce the wiring weight. Other factors in the realm of chemical, environmental, mechanical, thermal, electrical and physical also have effect on aircraft wiring.

The National Transportation Safety Board (NTSB) investigation reveals that it was the electrical wiring fault that caused the Boeing 747 TWA Flight 800 disaster in 1996 and the crash of a Swissair MD-11 in 1998 [2,3]. In addition, several aircraft incidents since then have resulted in emergency landings, power outages, on-board fires, etc., and were believed to happen due to electrical wiring fault. According to United States Navy reports [4,5], aircraft wiring faults were the originating issue in the following problems:

- Two in-flight fires every month;
- More than 1,077 mission aborts per year;
- More than 100,000 mission hours lost every year;

- One to two million man-hours per year for troubleshooting and repairing wiring issues.

The National Aeronautics and Space Administration (NASA) wiring safety program has identified that the arc fault (due to the damaged wires) as an issue of safety concern in many aircraft and space vehicles [6]. Hence, the research on early wiring fault detection and location methods has been increasing significantly. The traditional circuit breaker (TCB) can protect the load circuit from hard faults i.e., short circuits and overload currents. But, if the fault current is small or disappears in short duration due to vibrations or other reasons, the TCB cannot detect it, and the fault remains elusive.

Among wiring faults that could occur commonly in aircraft, intermittent arc faults (about 37 %) are the most frustrating, mysterious and extremely difficult to detect and locate in complex aircraft PDS because they can disappear in a few milliseconds due to vibrations or other reasons [4,5,7]. The detection and location of intermittent arc faults is very significant and has raised much concern in recent years, because they appear only under particular conditions, and evolve into serious permanent faults that may cause on-board fires, system damage, power interruptions or catastrophic incidents if not dealt with properly. There are several techniques to deal with intermittent arc faults [4,5,7-9]; however they require special devices such as transmitters, receivers, signal generators, dedicated sensors, etc., to detect and locate faults. This decreased their practicality for application in aircraft safety.

Recent trends in solid state power controllers (SSPCs) motivated the development of non-destructive diagnostic methods for health monitoring of aircraft wiring. The objective of this

thesis is to demonstrate the development of effective and non-destructive diagnostic methods for intermittent arc fault detection and location, for SSPC-based aircraft PDS.

This chapter is composed of six sections. The first section gives the overview of the chapter. The second section describes the different causes for wiring faults, including intermittent arc faults. The review of existing techniques and their applicability/practicability for intermittent arc fault detection and location are discussed in the third section. The SSPC-based aircraft DC PDS is presented in the fourth section. The fifth section provides the objectives and contributions of this thesis. In the last section, the outline of the thesis is described.

1.2 Causes of Wiring Faults

The electrical wire in aircraft is often coated with different insulating materials such as polyimide (PI), polytetrafluoroethylene/polyimide composite (CP) and polyvinylchloride (PVC)/nylon (PV) for safety concerns and appropriate function [10]. The aircraft wiring insulation can be degraded over a period of time due to numerous factors such as environmental, chemical, thermal, mechanical, electrical and physical issues [10,11].

The voids and scissions (or microscopic cracks) may develop due to aging or hydrolytic deterioration, and this phenomenon results in the electric field non-uniformity within insulators which leads to an insulation degradation [12]. Studies show that the PI and PV aircraft wires would have a higher risk of aging or degradation in the presence of high moisture [10]. High temperatures due to overload currents or faults are also an important aging factor that could directly influence the wire insulation. Though low temperatures cannot affect the aging of wire, it alters the insulation properties [10]. In the presence of mechanical vibrations or stresses, the wire can rub against the airframe or any metal structure, including another wire, connector, or

wire clamp, which may cause insulation to breach out, leading to a chafe/fray fault [10,13]. The overloads or faults can cause high currents, which may produce overheating and this phenomenon result in the accelerated aging of wire. The high voltage (above 1000 volts) causes the corona and partial discharges (PD) [10,12]. In addition, human errors (or physical errors) such as mishandling of wire, improper installation of wiring system/connector/wire clamp, etc., can also contribute to the wiring degradation. All of the above-mentioned aging factors and their effects are summarized in Table I.

Table 1.1 Aircraft wiring aging factors and their effects [10-13]

Aging factor		Effects
Thermal	High temperature due to overload currents or faults	Aging of wire, cracks in wire insulation, changes of insulation color, chemical reaction, etc.
	Low temperature	Effect of the insulation properties.
Environmental and chemical	Moisture, pressure, humidity, water, fluids/cleaners, oxidation, etc.	Corrosion, increased rigidity, cracks in insulation, water trees, accelerated aging, etc.
Mechanical	Vibration, bending, stresses, and force.	Chafing or abrasion, effects of insulation mechanical integrity, etc.
Electrical	High voltage (above 1000 volts)	Corona and partial discharges.
	Over currents due to overloads or faults	Additional temperature.

Fig. 1.1 shows the different causes of wiring faults that were found during routine maintenance and operations from 1980 to 1999 [2]. Among them, the chafed or damaged wire insulation (when it exposes the wire conductor) is one of the major root causes for short circuit and/or arcing related faults. This problem persists over a long time period only if not detected and paves the road for a serious fault, on-board fires and catastrophic incidents. The aircraft wiring system is usually located in harsh dynamic electrical environments which comprise moisture, vibration, mechanical stress, turning-on and turning-off of loads etc. During harsh in-flight vibrations, under mechanical stresses on the wires and when water drips on damaged wires or in the presence of moisture, the breached/degraded wire insulation can expose its conductor to the surrounding conductive material which causes an intermittent arc fault.

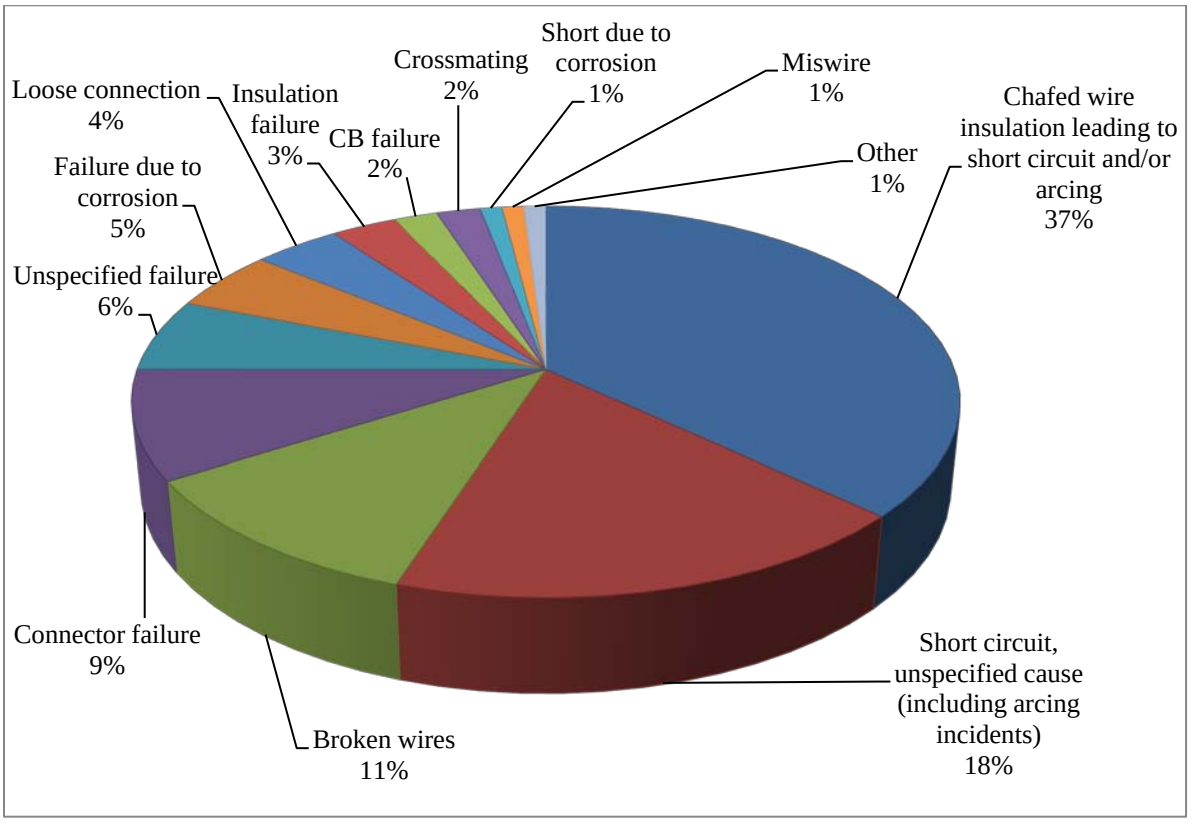

Fig. 1.1 Causes of wiring faults [2]

These faults occur with short duration and at low magnitudes. Basically the phenomenon cannot be repeated when the aircraft is back on the ground. In rare situations, intermittent arc may happen during harsh chafing fault evolution. Intermittent arc faults can be classified into two types as follows [4,5]:

- Dry intermittent faults: These appear under mechanical stresses or during in-flight vibrations;
- Wet intermittent faults: This can occur when water drips on damaged wires or in the presence of moisture.

1.3 Review of Existing Methods

In this section, several existing wiring fault detection and location systems, such as visual examination, end-to-end resistance measurement, reflectometry techniques, and power line communication approaches are examined. Also, dedicated sensors, i.e., acoustic, current, capacitance and inductance, traditional circuit breakers, arc fault circuit breakers, and aircraft load circuit modeling-based methods are reviewed and analyzed.

Visual Examination

Visual examination is a simple diagnostic method used to identify and/or locate the wiring faults such as chafes, cracks, holes in insulation, and signs of arc faults. Two types of wire samples, such as broken insulation, and wire with sign of arc, are shown in Fig. 1.2. Out of these, the damaged wire and type of fault can be identified at first glance.

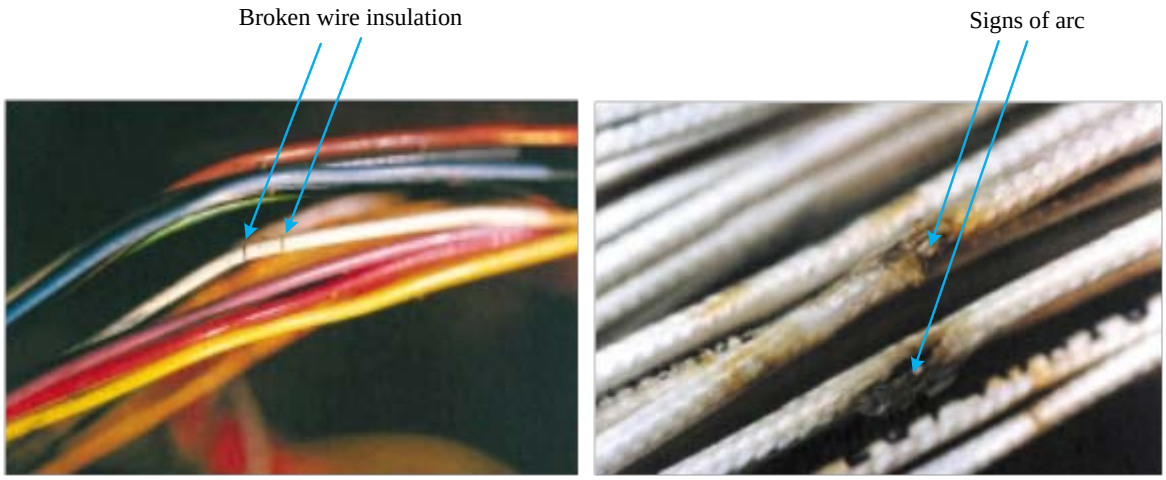

(a) Broken wire insulation (b) Signs of arc

Fig. 1.2 Wire samples; source: [3]

However, this method has the following drawbacks:

- The wiring faults, such as those in Figure 1.2, are hidden under clamps or aircraft walls, within bundles, and other places, and therefore cannot easily be found;
- Fault inspection requires twisting or turning the wire, which does more harm to the wire than good;
- This inspection also requires specially designed glasses to check the microscopic wiring faults;
- Furthermore, examination of an intermittent arc fault may not be suitable because the fault appears only under particular conditions;
- Moreover, visual examination is a tedious and time-consuming process.

End-to-end resistance measurement

If the end-to-end resistance is low, the wire is healthy [3,14] and a high resistance means that it is broken. However, this method suffers the following problems:

- The wire has to be disconnected from the circuit for measurement or testing, which isn't acceptable in field application;
- Chafe and intermittent faults remain undetectable.

Reflectometry technique

The reflectometry technique is a well-known diagnostic method commonly used for detection and location of wiring faults. This technique usually sends special designed signals such as step, square, rectangular and pseudo noise (PN) down the wire, and identifies the fault location by the analyzing incident and reflected signal. According to the type of incident signal, reflectometry techniques are classified into frequency domain reflectometry (FDR) [14], time domain reflectometry (TDR) [15], sequence time domain reflectometry (STDR) [16], spread spectrum time domain reflectometry (SSTDR) [16], etc.

The functional block diagram of TDR is shown in Fig. 1.3, in which step signal is used as the incident signal V_{inc} and the sampler circuit is employed for collection of reflected signal V_{ref} that is arrived at from a fault and/or load. The fault can be located by analyzing the time delay between the incident and reflected signal.

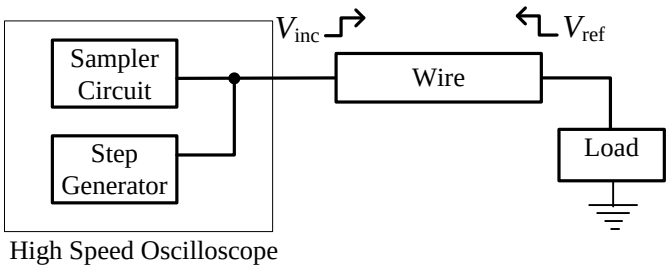

Fig. 1.3 Functional block diagram of TDR

With TDR, hard faults such as shorts and open circuits can easily be detected and located [15]. However, it is difficult to detect and locate chafe faults for the following reasons:

- A chafe fault (based on its severity) would make a small reflection when compared with the hard fault, because of tiny changes in wire impedance which are very difficult to collect and analyze in the presence of system background noise.
- Some deviations may occur in velocity of propagation because of continuous changing wire parameters such as permittivity and conductivity, which may affect the estimation accuracy of the fault location. [17].

Some further improvements are made for TDR in [17] with the *S*-parameters modeling method and Bayesian probabilistic inversion method. In this method, the wire, including the single chafe fault, is modeled with the *S*-parameters method. Then the inversion method is applied to obtain the fault location and size of fault. However, this method suffers with the computational burden and the slow process of output results (8 to 10 hours).

In phase detection frequency domain reflectometry (PDFDR), standing wave reflectometry (SWR) and mixed signal reflectometry (MSR), the arbitrary waveform generator (AWG) is

utilized to generate a set of stepped-frequency sine waves, which are used as incident signals. The coupler circuit is employed to separate the reflected signal from the incident signal. PDFDR locates the wiring fault by analyzing the phase difference between incident and reflected signals [14,15]. For estimation of fault location, SWR examines the peaks and nulls of the standing wave generated by the mixture of reflected and incident waveforms [14,15]. To reduce cost and achieve same performance as PDFDR and SWR, MSR is implemented in [18], where the main expensive component, the directional coupler, is eliminated. MSR requires a voltage-controlled oscillator, attenuator and a simpler mixer to mix the incident and reflected signal. It squares the mixed signal and analyzes the dc component of the mixed signal, to locate the fault. As in TDR, these reflectometry methods are also not feasible for chafe fault detection.

TDR, FDR, SWR, MSR, etc., are only suitable for ground maintenance after all aircraft loads disengaged, and they cannot be useful for live monitoring of wiring system because the special incident waves such as step, rectangular and square can disturb the original power flow. Hence, intermittent wiring faults that appear only during flying remain hard to discover.

Unlike TDR and other methods, STDR/SSTDR utilizes very low voltage sine wave modulated/digital PN code as an incident signal and it estimates the fault location by analyzing the correlation between the incident and reflected signals [4,5,16]. This method can be useful for in-flight wiring fault diagnosis because the PN code appears like a noise and may not disturb the actual electrical power. Based on the above significant technique, STDR and SSTDR have been used to practice tracking and locating intermittent arc faults when they are near short circuits, according to the reflections of pseudo noise (PN) signals injected onto the wire [4,5]. However, STDR and SSTDR methods have the following problems associated with them:

- To monitor the aircraft power wires continuously with PN signal, these methods require specially designed hardware such as non-contact capacitive probes [19], low-power STDR CMOS (complementary metal-oxide semiconductor) sensors [20], S/SSTDR ASIC (application specific integrated circuit) [4], etc. These specialized pieces of hardware increase the cost, weight and maintenance expenses.
- It is impractical to send, receive and analyze PN signals in a complex aircraft PDS.
- If the injected PN signals are very small, the collection and analysis of tiny reflected PN signal in presence of system background noise is difficult, which would affect the accuracy of estimations of intermittent fault location.
- On the other hand, if the PN signals are large, this may influence the original power already on the wire.
- In a dynamic aircraft PDS, switching variations such as turning-on and turning-off of the SSPC/aircraft load and load transients may also cause reflections which make these methods onerous.
- Because of continuous changing wire parameters, some deviations may occur in the velocity of propagation, which may affect the estimation accuracy of the fault location.
- The multiple reflections from the wiring junctions remain unsolved.

Power line communication

A power line communication (PLC) approach enables the device to send a carrier or other digital data signal through electrical wires. Both the electric current and carrier signal are usually run at different frequency levels, so that they do not influence each other. Accordingly,

intermittent fault identification method is proposed based on the carrier signal behavior [7]. In this manner, the carrier signal transmits at one location of the wire by using the transmitter and then, it would receive at another location of the wire by utilizing the receiver circuit. The receiver circuit cannot receive the carrier signal completely if the fault occurs during the time of carrier signal travelling and thus, the fault can be identified based on the error rate of the carrier signal. However, this method requires transmitters, receivers and coupling circuits at different locations on wire which holds their viability in aircraft.

In 2011, Honeywell patented a new diagnostic method called PLC-based aircraft PDS with real time wiring integrity monitoring capability [21]. This new approach enables a simple and effective platform for implementation of both PLC and SSTDR technologies in aircraft PDS, in order to achieve the following main functions:

- To monitor the aircraft wires continuously with PN code;
- Real time wiring fault detection and location by means of SSTDR;
- To control the remote power controller (RPC) or other protective devices with the PN code signal or other digital signal.

However, this approach increases the complexity of the aircraft PDS, and requires special devices such as signal generators, coupling circuits, dedicated sensors, transmitters, etc.

Protective devices

The thermal circuit breakers (TCBs) are used widely in various industries, houses, automobiles and other power systems. A TCB works based on a thermal sensitive element, and it

opens the circuit when a high enough steady fault current flows through an element for a sufficient amount of time. This has following drawbacks:

- It cannot detect intermittent arc because of inconsistent arc current [6] and short duration of fault;
- It is not enough for chafe fault detection because of the very small amount of fault current.

The arc fault circuit breaker (AFCB) can improve the safety of aircraft PDS by detecting the arc fault based on advanced electronics, special algorithms and pattern matching techniques [22]. This enables better protection than TCB. However, the AFCB is still used only in alternating current (AC) PDS [22] and does not provide any information about fault location.

Acoustic sensors

The acoustic wiring diagnostic system (AWDS) based on passive acoustic sensors is developed for detection and location of chafing and intermittent arc faults [8]. It incorporates many sensors on a wiring bundle to collect acoustic signals generated by wiring faults. However, this method may not be suitable for aircraft PDS due to the following problems:

- Acoustic sensors should be placed near to faults for efficient fault detection, and the location of sensors affects their practicability for aircraft PDS;
- Furthermore, the noise caused by the flight vibrations may affect the output of sensors;
- All the acoustic sensors should be tied into a special network for fault examination which increases the installation cost and maintenance expenses.

Current sensors

When fault occurs, the unwanted fault current I_{fault} flows from the wire to the ground as shown in Fig. 1.4. Two current sensors (CS's) are placed on the wire to measure the current at different locations. Because of the fault, I_2 (measured current of CS 2) would not equal to I_1 (measured current of CS 1). Hence, the fault can be detected.

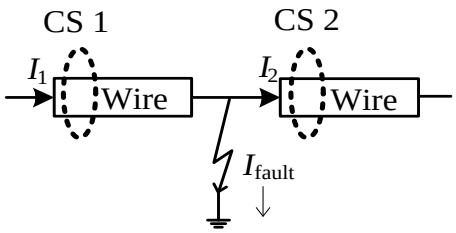

Fig. 1.4 Principal diagram of current sensor-based diagnostic method

According to this principle, the diagnostic method in [9] is able to detect and locate sparking or arc discharge based on measurement of the current flow difference between two adjacent current sensors. However, this method suffers the following drawbacks:

- Requirement for multiple current sensors at different locations on the aircraft wiring system which increases the cost and weight;
- Furthermore, all current sensors should be coupled with special connections for fault analysis, which enhances the complexity, cost and computational burden.

Inductance and capacitance sensors

The length of open-circuited wire is proportional to its capacitance and the length of short-circuited wire is proportional to its inductance [23]. Accordingly, a cost-effective solution by

means of capacitance and inductance sensors was developed for detection of open and short circuits [23]. The different sensors, such as the voltage divider, Schmitt trigger oscillator, 555 timer, differential amplifier, etc., are practiced for open and short circuit fault examination. Among these, the 555 timer and the differential amplifier sensors show better performance. However, these methods suffer the following problems:

- The additional inductance or capacitance caused by metallic components or other sources on unshielded wires, may impact the output of the sensors;
- These processes are not feasible for detection of faults on branched wires.
- They are not suitable for in-flight wiring health monitoring, and thus intermittent fault detection is still incomplete.

Diagnostic methods based on load circuit modeling

Arc fault detection based on model reference estimation is proposed in [24], where the aircraft load circuit is modeled with autoregressive (AR) method. This method estimates the load model with minimum error under normal working conditions based on preceding voltage and current samples; but it fails to define the model under arc fault conditions which are used as indicators for arc fault. This method focuses only on AC PDS static arc faults. However, it cannot give any information about fault location and may not be feasible for intermittent arc fault detection.

An approach for parallel wiring fault evaluation based on RLCG (resistance *R*, inductance L, capacitance *C*, and conductance *G*) load circuit modeling and parameter identification is proposed in [25]. In this paper, aircraft load circuits including single parallel wire faults are

modeled with cascaded T-type equivalent circuits and then, the transfer function coefficients and fault-related parameters are estimated with the utilization of step and white noise excitations. Simulation results show that fault can be identifiable with white noise excitation. However, this method should be modified or improved further in order to detect and locate intermittent wiring faults.

1.4 SSPC-Based Aircraft DC PDS

Power electronics have received wide acceptance from industries, consumers and researchers because of the ability to work with high power ratings, reliability, controllability, smaller size, etc. This exceptional technology enables the development of innovative and significant protective devices, i.e., solid state power controllers for aircraft and other vehicle electric PDS. SSPC devices have received enormous attention in modern aircraft PDS because of their prominent features [22,26], such as:

- Simple design and reliability.
- Smaller size and lower weight.
- The ability to provide instant trip capability (about 25 microseconds) [6] under fault conditions because they are based on power switching devices such as metal oxide semiconductor field effect transistors (MOSFET), insulated gate bipolar transistors (IGBT), etc.
- Remote control capability by means of special signals or preprogrammed software.
- The capability of accessing the voltage and current of the load circuit using sensors.
- The ability to work with 270V DC and high power levels.

- Because of its small size, SSPC can be placed near loads to minimize the wire length and gauge.
- Furthermore, it can be extended further to meet special requirements, i.e., health monitoring of wiring systems via advanced electronics, data acquisition systems (DAS), pattern matching of normal working currents and advanced algorithms.

An SSPC-based aircraft DC PDS is shown in Fig. 1.5, where, SSPC plays a key role by serving two important functions:

1) Safe connection of aircraft loads to respective power bus, and

2) Providing protection from abnormal events such as overloads, short circuits, arc faults, etc.

The main generated power is initially converted into 270V DC to support the high power loads and to increase the reliability. Then it would be converted into 28V DC and 115V AC to feed local aircraft loads. Furthermore, all SSPCs in PDS can be controlled with an intelligent power controller which enhances the reliability and safety.

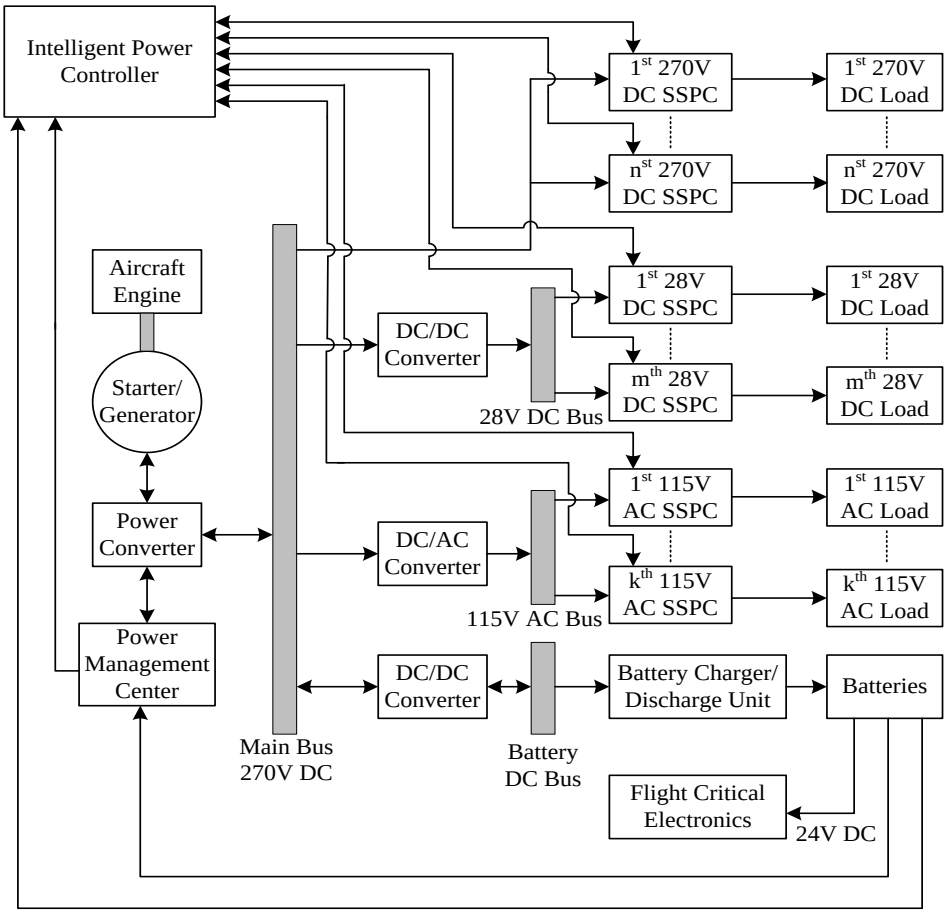

Fig. 1.5 An SSPC based aircraft DC PDS

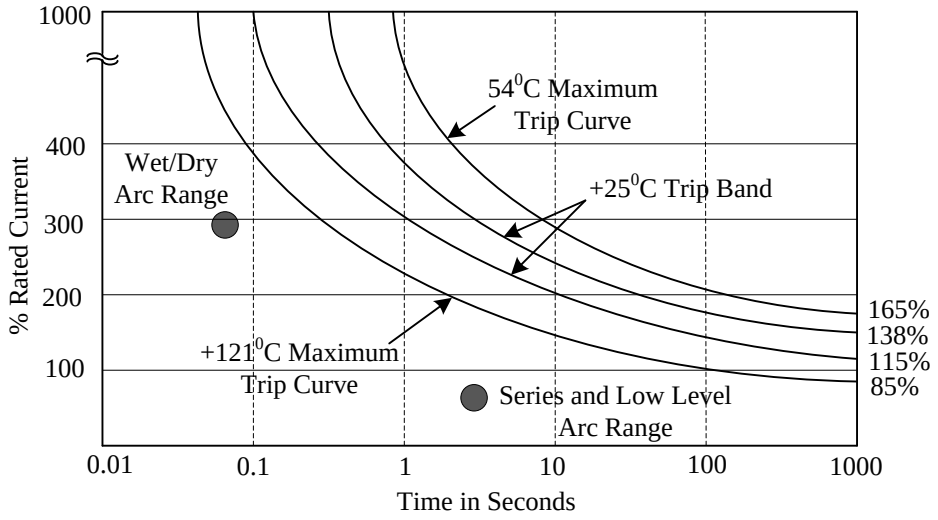

Fig. 1.6 Typical I^2t trip characteristics [27]

SSPC's have similar I^2t trip characteristics of TCB as shown in Fig. 1.6. Wet/dry arcs would create a 300% rated current, but this disappears in a short period (less than 1 second). Series and low level arcs cause less current, but stay for long time periods (about 1 to 5 seconds). According to typical I^2t trip characteristics, the fault should make at least 10 times of rated current or stay for a long duration to trip the circuit instantly. On the other hand, lowering the threshold may raise the wrong trips or false alarms. Therefore, SSPCs requires the most intelligent algorithms to detect and locate the intermittent arc faults.

In 2007, Honeywell patented a new diagnostic method called arc fault detection for SSPC-based electrical power distribution systems [26]. This method provides an additional feature i.e., arc fault detection method, for SSPC, by comparing the measured load current with the reference load current. This reference load current is usually obtained from the learning/testing process and is then stored in the internal memory for fault inspection. However, it is designed only for AC PDS faults and cannot give any information about fault location.

1.5 Thesis Objectives and Contributions

The existing techniques generally require injections of small signals and associated external devices such as transmitters, receivers and dedicated sensors, which hold their viability for aircraft application. An ideal intermittent wiring fault diagnostic method must meet the following three key objectives:

1. **Non-destructive:** The diagnostic method should not harm the original power already in the wire.

2. **Simple yet accurate:** The diagnostic method should be simple in terms of computation and practical implementation, and it should be able to detect and locate faults accurately.
3. **Live monitoring:** Intermittent arc faults appear only under particular conditions, in unpredictable manners, and they cannot repeat when the flight is back on the ground. Hence, the diagnostic method should be able to monitor the wiring system in a real-time manner for fault detection and location.

To sustain the above objectives, this thesis proposed an effective and non-destructive diagnostic method to detect and locate intermittent arc faults. Unlike the existing techniques which generally require special devices, the proposed method only needs circuit voltage and current measurement as inputs at the source end, and is thus suitable for SSPC-based aircraft PDS, in which voltage and current signals can be conveniently obtained.

The ABCD method can provide a transmission matrix which is also called an ABCD matrix [28]. With this ABCD matrix (where, *A*, *B*, *C* and *D* are called the coefficients), the relation between the input voltage and current, and output voltage and current, of a two-port network can be described. The *A*, *B*, *C* and *D* coefficients of an ABCD matrix depend on the transmission line parameters and the type of load.

The main contributions of this thesis are as follows:

- The ABCD method is introduced to derive normal and faulty aircraft load circuits with reduced complication and a potential of higher accuracy compared to the conventional differential equation approach. With this method, the complex load

circuits can be modeled by representing each section, i.e., wire segment/load/fault with an individual ABCD matrix, which improves the reliability and accuracy.

- A simple yet efficient method for intermittent arc fault detection is proposed based on the estimation of normal load circuit model coefficients and wiring parameters. Intermittent arc faults can cause broadband frequency disturbance and voltage dips (or voltage sags). This phenomenon causes temporary deviations in the model coefficients and wiring parameters, which can be regarded as an indicator of fault occurrence.
- The fitness function is formulated for estimation of fault-related parameters, such as intermittent arc location and average intermittent arc resistance, based on the faulty load circuit modeling and its coefficients.
- A genetic algorithm (GA) is proposed to minimize the formulated fitness function which leads to an optimal estimation of fault-related parameters.
- The proposed methods are verified by simulations and experiments using a 28V DC power supply. Dry line-to-ground intermittent arcs are simulated in the lab by vibrating the chafed wire against the ground which mimics the aircraft environment. The robustness of these proposed methods will also verify with the switching events such as turning-on and turning-off of load circuits.

1.6 Thesis Outline

This thesis consists of five chapters. Chapter 1 provides the introduction to the thesis, where different causes of wiring faults are outlined, and a review of existing methods is made, including TDR, STDR/SSTDR, carrier-based PLC, etc. In addition, SSPC-based aircraft DC

PDS, and the objectives, contributions and the outline of the thesis are given. Chapter 2 deals with the aircraft load circuit modeling, which comprises five sections. The overview and introduction of ABCD method are discussed in the first and second sections, respectively. Section 3 describes the modeling of the normal load circuit based on the ABCD method. Practical issues and faulty load circuit modeling are discussed in section 4, and chapter 2 is summarized in section 5. In chapter 3, the proposed methods for model coefficients and wiring parameter's estimation, intermittent arc fault detection, and GA-based fault location estimations are provided. Simulation and experimental results under different test conditions such as turning-on/-off of load circuit, normal and fault conditions are discussed in chapter 4. The conclusions and future work are given in chapter 5.

CHAPTER 2

AIRCRAFT LOAD CIRCUIT MODELING

2.1 Overview

The feasibility of intermittent arc fault detection and location can be accomplished by an efficient and accurate modeling of a normal and faulty load circuit. There are several ways to model the load circuits, such as the differential equation approach, autoregressive (AR) method, etc. The differential equation approach is used to model faulty transmission and distribution power systems for estimation of fault locations [29]. AR technique is used in [24] to model the aircraft linear normal load circuits. However, these methods are associated with such problems as lack of reliability and computational inefficiency. Therefore, the ABCD matrix modeling method is introduced to model the typical aircraft load circuits. With this method, the complexity of load circuit modeling can be reduced by representing each section, whether it is a wire segment or load or fault, with an individual ABCD matrix. Hence, this method improves the reliability and accuracy. Furthermore, it is capable of modeling frequency dependent parameters and reactive loads [28].

This chapter consists of five sections. The first section gives the overview. In the second section, the ABCD method is introduced with explanation of how it can model the complex systems. The mathematical modeling of aircraft normal load circuits is provided in the third section. The electrical characteristics of intermittent arc faults and aircraft faulty load circuit modeling are described in the fourth section. Finally, the fifth section is a summary.

2.2 ABCD Method

The ABCD method is accurate, and flexible to model the complex aircraft load circuits. A simple two-port electrical network *m* is shown in Fig. 2.1. V_1 and I_1 represent the input voltage and current of the two-port network *m*, respectively and V_2 and I_2 represent the output voltage and current of two-port network *m*, respectively. The relationship between the input voltages V_1 and current I_1, and output voltage V_2 and current I_2, of a two-port network *m* can be described with an ABCD matrix as follows:

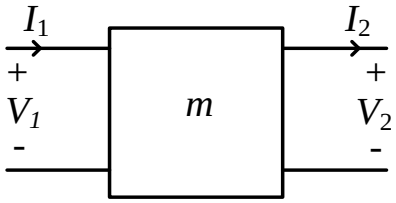

Fig. 2.1 A simple two-port network

$$\begin{bmatrix} V_1 \\ I_1 \end{bmatrix} = m \times \begin{bmatrix} V_2 \\ I_2 \end{bmatrix}, \tag{2.1}$$

where

$$m = \begin{bmatrix} A & B \\ C & D \end{bmatrix}. \tag{2.2}$$

and where *A*, *B*, *C*, and *D* are called the coefficients. They depend on the wire parameters, fault and the type of load, and should be derived according to electrical circuit theory. An n-section cascaded two-port network is shown in Fig. 2.2. V_1 and I_1 represent the input voltage and current of two-port network m_1, respectively, V_2 and I_2 represent the input/output voltage and current of

two-port network m_2/m_1, respectively, V_3 and I_3 represent the output voltage and current of the two-port network m_2, respectively. Then V_{n-1}, I_{n-1}, V_n and I_n depicts the input voltage, input current, output voltage and output current of a two-port network m_n, respectively. The overall response of an n-section cascaded two-port network as shown in Fig. 2.2 can be obtained as follows:

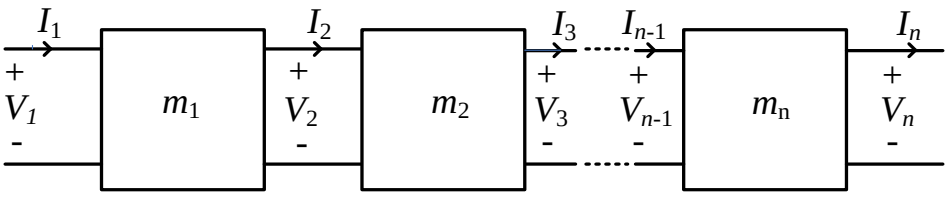

Fig. 2.2 An n-section cascaded two-port network

$$\begin{bmatrix} V_1 \\ I_1 \end{bmatrix} = (m_1 \times m_2 \times \cdots \times m_n) \times \begin{bmatrix} V_n \\ I_n \end{bmatrix}, \tag{2.3}$$

where

$$m_1 = \begin{bmatrix} A_1 & B_1 \\ C_1 & D_1 \end{bmatrix}, \tag{2.4}$$

$$m_2 = \begin{bmatrix} A_2 & B_2 \\ C_2 & D_2 \end{bmatrix}, \tag{2.5}$$

……,

$$m_n = \begin{bmatrix} A_n & B_n \\ C_n & D_n \end{bmatrix}. \tag{2.6}$$

The ABCD method is able to model the complex or cascaded electrical circuits by representing each section, whether it is fault or wire or load, with an individual ABCD matrix. It then combines all individual ABCD matrix's to get the overall response of the system.

2.3 Modeling of Normal Load Circuit

The aircraft wire possesses the four fundamental parameters such as resistance, inductance, shunt capacitance and shunt conductance. Each wire has some resistance, *R* which opposes the flow of current. The resistance of the wire can be represented by following:

$$R = \rho \frac{l}{a} \ \Omega/\text{m} \tag{2.7}$$

where, ρ is conductivity of wire; *l* is length of wire in meters; and *a* is the cross-sectional area of the wire. The wire resistance *R* may rise when the wire diameter reduces due to crushing, stretching and corrosion. In actuality, no wire is ideal and there is always some leakage current which flows through the insulation. The wire insulation generally works as dielectric; here, insulation acts as a resistor which causes a very small leakage current. The shunt conductance *G* can be neglected when the leakage current is too small. The inductance *L* and capacitance *C* of two-wire transmission line can be given by Equations 2.8 and 2.9 [23]:

$$L = \frac{\mu}{\pi} \cosh^{-1}\left(\frac{D}{2a}\right) \quad \text{H/m} \tag{2.8}$$

$$C = \frac{\pi\varepsilon}{\cosh^{-1}\left(\frac{D}{2a}\right)} \quad \text{F/m} \tag{2.9}$$

where the two wires are separated by a distance D in a dielectric medium (ε, μ) and a is the radius of wire. The inductance can be influenced by the diameter of wire and magnetic permeability. The capacitance of wire depends on the type of insulation, distance between wires and the permeability of the dielectric medium, and it increases when wires are separated during rubbing or vibrations.

Aircraft wire can be modeled as a transmission line with the resistance, inductance, capacitance and conductance [30,31]. The ABCD method can be used to model a branched aircraft wiring network as in [28]. In this thesis, a typical aircraft load circuit including wire segments, fault and load is considered as a cascaded two-port network, and the parameters of the two-port networks are represented by 2×2 matrices, i.e., ABCD matrices. To simplify operations, the load will also be regarded as a two-port network with zero output current.

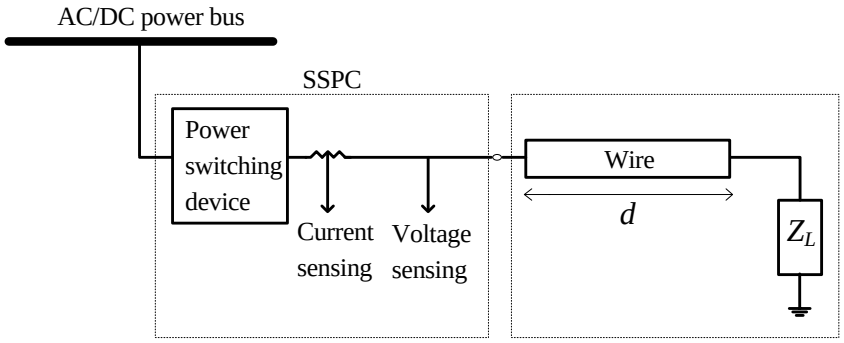

Fig. 2.3 SSPC-based normal load circuit.

The model of a typical SSPC-based load circuit under normal conditions is shown in Fig. 2.3, in which the impedance of the load is denoted as Z_L and d represents the wire length in meters. The power bus provides either AC (115V, 400Hz) or DC (28/270V) power to the load. The SSPC connects the load circuit to the power bus in a safe manner and protects the load

circuit from faults or overloads based on typical I^2t trip characteristics. The voltage and current sensors contained in the SSPC can be used to measure circuit voltage and current, respectively [26].

An RLCG-based wire model is developed in Fig. 2.4. The effect of mutual inductance and capacitance are not considered. I_{1n} and V_{1n} represent the current and voltage that are measured within SSPC, respectively. Practically, no wire is ideal and there is always some leakage current that flows through insulation. I_{2n} and V_{2n} may represent the leakage current of the wire and the induced voltage drop respectively. I_{3n} and V_{3n} represent the input/output current and voltage of the two-port network m_{2n}/m_{1n}. I_{4n} and V_{4n} represent the load current and voltage respectively. I_{5n} and V_{5n} represent the output current and voltage of m_{2n}. The r, l, c, and g are the resistance, inductance, shunt capacitance and shunt conductance of the wire per meter length respectively. The $z = r + sl$ and $y = g + sc$ are the series impedance and shunt admittance of the wire per meter length.

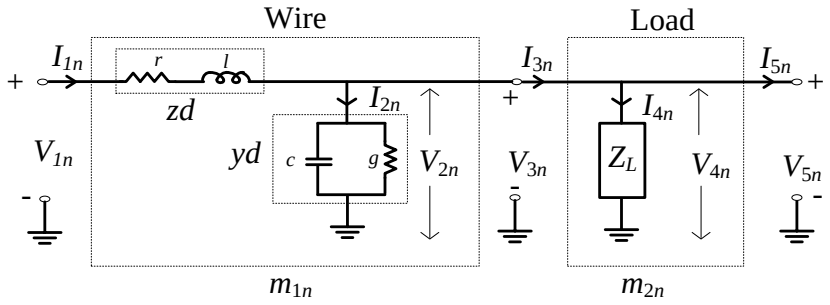

Fig. 2.4 Model of normal load circuit.

The response of the two-port electrical network m_{1n} shown in Fig. 2.4 can be obtained based on the circuit theory as follows:

$$\begin{bmatrix} V_{1n} \\ I_{1n} \end{bmatrix} = m_{1n} \times \begin{bmatrix} V_{3n} \\ I_{3n} \end{bmatrix}, \tag{2.10}$$

where

$$m_{1n} = \begin{bmatrix} A_{1n} & B_{1n} \\ C_{1n} & D_{1n} \end{bmatrix} = \begin{bmatrix} 1+zyd^2 & zd \\ yd & 1 \end{bmatrix}, \tag{2.11}$$

Similarly, the response of the two-port electrical network m_{2n} shown in Fig. 2.4 can be obtained as follows:

$$\begin{bmatrix} V_{3n} \\ I_{3n} \end{bmatrix} = m_{2n} \times \begin{bmatrix} V_{5n} \\ I_{5n} \end{bmatrix}, \tag{2.12}$$

where

$$m_{2n} = \begin{bmatrix} A_{2n} & B_{2n} \\ C_{2n} & D_{2n} \end{bmatrix} = \begin{bmatrix} 1 & 0 \\ \dfrac{1}{Z_L} & 1 \end{bmatrix} \tag{2.13}$$

The two-port networks m_{1n} and m_{2n} are then integrated to obtain the overall response of the normal load circuit, which can be shown by

$$\begin{bmatrix} V_{1n} \\ I_{1n} \end{bmatrix} = m_n \times \begin{bmatrix} V_{5n} \\ I_{5n} \end{bmatrix}, \tag{2.14}$$

where

$$m_n = m_{1n} \times m_{2n} = \begin{bmatrix} A_n & B_n \\ C_n & D_n \end{bmatrix} = \begin{bmatrix} 1 + zyd^2 + \dfrac{zd}{Z_L} & zd \\ yd + \dfrac{1}{Z_L} & 1 \end{bmatrix}. \tag{2.15}$$

Equation (2.14) can be rewritten as:

$$V_{1n} = A_n V_{5n} + B_n I_{5n}, \tag{2.16}$$

$$I_{1n} = C_n V_{5n} + D_n I_{5n}, \tag{2.17}$$

where I_{5n} is always equal to zero, and V_{5n} equals to V_{3n}. Therefore the two-port network m_{2n} can be treated as a unity matrix [8]. Thus Equations (7) and (8) can be rewritten as:

$$V_{1n} = A_n V_{3n}, \tag{2.18}$$

$$I_{1n} = C_n V_{3n}, \tag{2.19}$$

Then, the input impedance Z_{1n} of the load circuit can be obtained:

$$Z_{1n} = \frac{V_{1n}}{I_{1n}} = \frac{A_n}{C_n}. \tag{2.20}$$

This input impedance equation relates the wiring and load parameters directly to the load circuit input voltage and current measurements.

2.4 Modeling of Faulty Load Circuit

Intermittent arc faults commonly appear in aircraft when the damaged wire exposes its conductor to surrounding conductive material during flight vibrations or under mechanical stresses. The estimation of intermittent arc location is very significant, because it is not possible to reproduce on the ground. To estimate the location of the intermittent arc fault accurately, the faulty load circuit including the intermittent arc should be modeled properly based on its characteristics.

An electric arc characterization can be analyzed using the anode, cathode and plasma columns as shown in Fig. 2.5. The anode and cathode could be any damaged wire or conductive material or electrode. No arc current I_{arc} flows from anode to cathode when there is sufficient distance between them. But, when they come together during vibrations or under mechanical stresses, arc current I_{arc} begins to flow. The amount of arc current I_{arc} that is flowing from anode to cathode and arc voltage V_{arc}, i.e., the voltage of the plasma column, are dependent on plasma column resistance (or arc resistance R_{arc}).

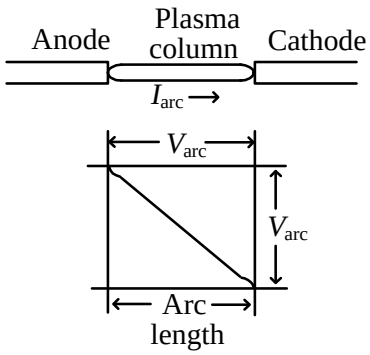

Fig. 2.5 Electric arc characterization [32]

To make the representation very clear in this thesis, the anode is considered as a positive wire and the cathode is considered as a ground. In static arc fault conditions, the plasma column can be fully energized, which results in a chaotic current flow between the positive wire and the ground. Under these conditions, the relationship between arc current, arc voltage and arc resistance becomes more complex, which makes the modeling of the arc more difficult.

If the positive wire fluctuates against the ground caused by in-flight vibrations, the arc resistance R_{arc} would also vary proportionally to the changes in arc length. Consequently, the arc current and arc voltage can alter rapidly with respect to the rate of change of arc resistance R_{arc}. Furthermore, the intermittent arc depends on the following factors:

- Type of insulation [6]: polyimide insulation may be sensitive to arc tracking faults.
- Surrounding conditions: wet arcs can happen when water drips on damaged wires and dry arcs can occur during vibrations or under stresses.
- Load circuit voltage and current ratings: the arc may show different characteristics at different current levels [32].
- Duration of arc: chaotic current can flow through a plasma column, if arc is static.

The modeling of the static arc based on particular test conditions for a DC system is given in [32]. However, the modeling of an intermittent arc, based on certain presumptions such as arc length, arc current, electrode material, test voltage, etc., may not be suitable in our case, especially if the fault location estimation is one of the objectives. There are two key issues:

1. Certain presumptions in modeling may not be applicable at all field conditions because intermittent arc fault occurs in unpredictable manners when the damaged

wire exposes the conductor to the surrounding conductive material during in-flight vibrations or under mechanical stresses, etc., and

2. Certain presumptions in modeling may cause large deviations in the estimation of fault locations which cannot be acceptable for aircraft application because of the small wire lengths when compared to transmission and distribution power line lengths.

During intermittent arc evolution, the arc resistance R_{arc} can fluctuate very rapidly because of the changing intermittent arc length. This can cause inconsistent arc current I_{arc} flow between two conductors or one conductor and the ground. This phenomenon results in the following two important features:

- The curves in Fig. 2.6 illustrate the scenario that voltage drops to a certain value due to an intermittent arc fault, and, then, it gradually recovers back to its actual value.
- A disturbance in the broadband frequency spectrum of voltage and current.

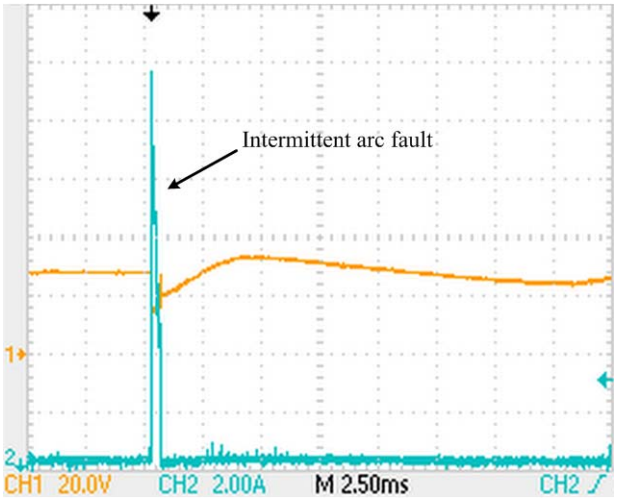

Fig. 2.6 Input voltage and current of load circuit during a typical intermittent arc fault condition

After fault, the load circuit would behave normally as if nothing happened previously. In some situations, such as during rapid vibrations, intermittent arcs may disappear in a short period of time, as shown in Fig. 2.6. Under these conditions, its behavior is near to short-circuit rather than chaotic over that short time period (about a few milliseconds) [31]. This makes it possible to model an intermittent arc which can be represented by a variable non-linear arc resistance R_{arc} implicating the stochastic arc current that flows from the damaged wire to the ground as shown in Fig. 2.7 and Fig. 2.8 [31]. This representation is sufficient when the objective is to find the arc location. As mentioned previously, the arc resistance equation based on certain presumptions such as arc length and arc current is not applicable at all field conditions because of unpredictable natures of intermittent arc faults. In Fig. 2.7, d_1 denotes the distance of the fault location from the SSPC and d_2 is that from the load end.

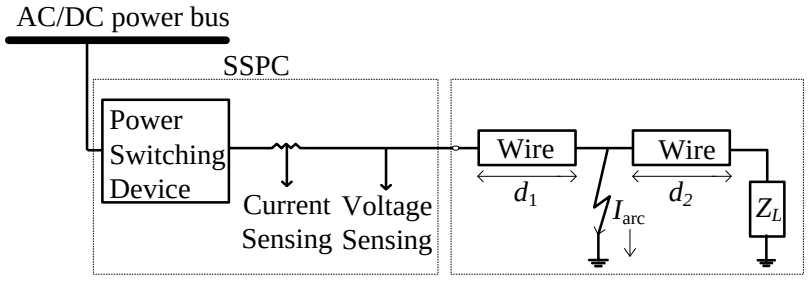

Fig. 2.7 SSPC-based faulty load circuit.

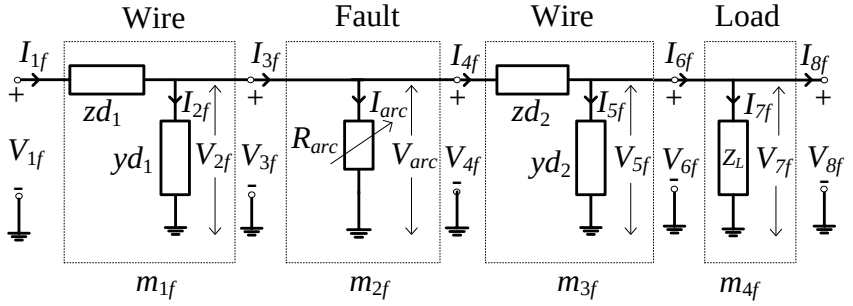

Fig. 2.8 Model of faulty load circuit.

In Fig 2.8, I_{1f} and V_{1f} represent the current and voltage that are measured within the SSPC, respectively. I_{2f}/I_{5f} and V_{2f}/V_{5f} depict the leakage current of m_{1f} and m_{3f} wire segments and the induced voltage drops, respectively. I_{3f} and V_{3f} represent the input/output current and voltage of the two-port network m_{2f}/m_{1f}, respectively. I_{arc}, V_{arc} and R_{arc} depict the arc current, arc voltage and arc resistance respectively. I_{4f} and V_{4f} represent the input/output current and voltage of the two-port network m_{3f}/m_{2f}, respectively and I_{6f} and V_{6f} represent the input/output current and voltage of two-port network m_{4f}/m_{3f}, respectively. I_{7f} and V_{7f} represent the load current and voltage respectively. I_{8f} and V_{8f} represent the output current and voltage of m_{4f}, respectively. The definitions of z and y are the same as in section 2.3.

The response of the two-port electrical network m_{1f} shown in Fig. 2.8 can be obtained based on circuit theory as follows:

$$\begin{bmatrix} V_{1f} \\ I_{1f} \end{bmatrix} = m_{1f} \times \begin{bmatrix} V_{3f} \\ I_{3f} \end{bmatrix}, \tag{2.21}$$

where

$$m_{1f} = \begin{bmatrix} A_{1f} & B_{1f} \\ C_{1f} & D_{1f} \end{bmatrix} = \begin{bmatrix} 1+zyd_1^{\,2} & zd_1 \\ yd_1 & 1 \end{bmatrix}. \tag{2.22}$$

Similarly, the response of the two-port electrical network m_{2f} shown in Fig. 2.8 can be given by

$$\begin{bmatrix} V_{3f} \\ I_{3f} \end{bmatrix} = m_{2f} \times \begin{bmatrix} V_{4f} \\ I_{4f} \end{bmatrix}, \tag{2.23}$$

where

$$m_{2f} = \begin{bmatrix} A_{2f} & B_{2f} \\ C_{2f} & D_{2f} \end{bmatrix} = \begin{bmatrix} 1 & 0 \\ \frac{1}{R_{arc}} & 1 \end{bmatrix}. \tag{2.24}$$

Similarly, the response of the two-port electrical network m_{3f} shown in Fig. 2.8 can be represented by:

$$\begin{bmatrix} V_{4f} \\ I_{4f} \end{bmatrix} = m_{3f} \times \begin{bmatrix} V_{6f} \\ I_{6f} \end{bmatrix}, \tag{2.25}$$

where

$$m_{3f} = \begin{bmatrix} A_{3f} & B_{3f} \\ C_{3f} & D_{3f} \end{bmatrix} = \begin{bmatrix} 1+zyd_2^{\,2} & zd_2 \\ yd_2 & 1 \end{bmatrix}. \tag{2.26}$$

Similarly, the response of the two-port electrical network m_{4f} shown in Fig. 2.8 can be given by:

$$\begin{bmatrix} V_{6f} \\ I_{6f} \end{bmatrix} = m_{4f} \times \begin{bmatrix} V_{8f} \\ I_{8f} \end{bmatrix}, \tag{2.27}$$

where

$$m_{4f} = \begin{bmatrix} A_{4f} & B_{4f} \\ C_{4f} & D_{4f} \end{bmatrix} = \begin{bmatrix} 1 & 0 \\ \frac{1}{Z_L} & 1 \end{bmatrix}. \tag{2.28}$$

The two-port networks m_{1f}, m_{2f}, m_{3f} and m_{4f} are then integrated to get the overall response of the faulty load circuit, which can be shown by:

$$\begin{bmatrix} V_{1f} \\ I_{1f} \end{bmatrix} = m_{1f} \times m_{2f} \times m_{3f} \times m_{4f} \times \begin{bmatrix} V_{8f} \\ I_{8f} \end{bmatrix}, \tag{2.29}$$

Equation (2.29) can be rewritten as:

$$\begin{bmatrix} V_{1f} \\ I_{1f} \end{bmatrix} = m_f \times \begin{bmatrix} V_{8f} \\ I_{8f} \end{bmatrix}, \tag{2.30}$$

where

$$m_f = m_{1f} \times m_{2f} \times m_{3f} \times m_{4f} = \begin{bmatrix} A_f & B_f \\ C_f & D_f \end{bmatrix}. \tag{2.31}$$

Similar to Equation (2.20), the input impedance of the load circuit with faulty wire can be written as:

$$Z_{1f} = \frac{V_{1f}}{I_{1f}} = \frac{A_f}{C_f}, \tag{2.32}$$

where

$$A_f = \left.\begin{array}{l} 1 + yzd_2^2 + \dfrac{zd_2}{Z_L} + yzd_1^2 + y^2z^2d_1^2d_2^2 + \dfrac{yz^2d_1^2d_2}{Z_L} + \dfrac{zd_1}{R_{arc}} \\ + \dfrac{z^2yd_1d_2^2}{R_{arc}} + \dfrac{z^2d_1d_2}{Z_LR_{arc}} + zyd_1d_2 + \dfrac{zd_1}{Z_L} \end{array}\right\}, \tag{2.33}$$

$$C_f = \left\{ \begin{array}{l} yd_1 + y^2 z d_1 d_2^2 + \dfrac{yzd_1 d_2}{Z_L} + \dfrac{1}{R_{arc}} + \dfrac{yzd_2^2}{R_{arc}} + \dfrac{zd_2}{R_{arc} Z_L} \\ + yd_2 + \dfrac{1}{Z_L} \end{array} \right\}. \quad (2.34)$$

The ABCD method eliminates the unnecessary parameters such as B_f and D_f to evaluate the input impedance equation of the faulty load circuit. This gives the potential to model complex systems with the reduced complexity. Equation 2.32 relates the wiring, load and faulty parameters directly to the load circuit input voltage and current measurements.

2.5 Summary

This chapter addressed the ABCD matrix (or transmission matrix) modeling method, normal load circuit modeling, and faulty load circuit modeling based on the ABCD method. Intermittent arc faults in direct current (DC) power distribution system (PDS) can cause the voltage sags or dips and the broadband frequency disturbance. Based on this, the fault can possibly be distinguished from normal load circuit variations. According to the deduction of input impedance equations in section 2.3 and section 2.4, the ABCD matrix modeling method reduces the complexity of wire modeling compared to the traditional differential equation approach by representing each wire segment and load with cascaded two-port networks. However this approach works with high accuracy. Based on the established load circuit models, effective algorithms are introduced to detect and locate intermittent fault, which will be illustrated in the next chapter.

CHAPTER 3

INTERMITTENT ARC FAULT DETECTION AND LOCATION

3.1 Overview

Detection of intermittent arc fault from normal aircraft load circuit variations, such as turning-on and turning-off of load, and approximate fault location estimations are very significant. They usually appear only under particular conditions and would cause serious incidents if not dealt with properly. Hence, effective algorithms are introduction in this chapter to deal with complex intermittent arc faults.

This chapter is divided into four sections. The overview is given in the first section. The estimation method for normal model coefficients and wiring parameters, and intermittent arc fault detection methods are described in the second section. The fitness function formulization and genetic algorithm (GA) based fault location estimation method are provided in the third section. This chapter is summarized in the last section.

3.2 Model Coefficients and Wiring Parameters Estimation and Intermittent Arc Fault Detection

A solid state power controller (SSPC) can provide the information of input voltage and current by using voltage and current sensors, respectively. Based on the available voltage and current measurements, the load circuit model coefficients and wiring parameters can be estimated. To do so, the input impedance Equation (2.20) should be modified. For the normal

load circuit model demonstrated in Fig. 2.4, the transfer function of the load system with resistive load can be represented as follows, according to Equation (2.20):

$$\frac{1}{Z(s)} = \frac{I(s)}{V(s)} = \frac{b_1 s + b_0 + 1}{a_2 s^2 + a_1 s + a_0}, \tag{3.1}$$

where $Z(s)$, $I(s)$ and $V(s)$ are Laplace transform of input impedance, current and voltage respectively and coefficients of Equation (3.1) can be defined according to Equation (2.20) as follows:

$$a_0 = rd + R_L + rgR_L d^2 , \tag{3.2}$$

$$a_1 = crR_L d^2 + lgR_L d^2 + ld, \tag{3.3}$$

$$a_2 = lcR_L d^2, \tag{3.4}$$

$$b_0 = gR_L d, \tag{3.5}$$

$$b_1 = cR_L d , \tag{3.6}$$

where R_L represents the load resistance, and r, l, c, g, and d are the same as in the previous chapter. As described in chapter 2.4, intermittent arc fault causes the broadband frequency disturbance in voltage and current. Therefore, the measured input voltages and currents signals are analyzed in the frequency domain, in order to attain comprehensive effects of the intermittent arc. Operating in frequency domain, Equation (3.1) can be rewritten as follows [31,33];

$$V(j\omega_i) = I(j\omega_i)a_2(j\omega_i)^2 + I(j\omega_i)a_1(j\omega_i) + I(j\omega_i)a_0 - V(j\omega_i)b_1(j\omega_i) - V(j\omega_i)b_0\Big\}, \quad (3.7)$$

where $j\omega_i$, $V(j\omega_i)$ and $I(j\omega_i)$ (i = 0, 1, 2,..., N) represent the complex angular frequency, voltage and current at i^{th} frequency point respectively. Equation (3.7) represents the load system under normal conditions; when an intermittent fault occurs, the induced broadband frequency disturbance and sudden changes in voltage and current would cause deviation of the model coefficients and wiring parameters from the normal ones, which can be regarded as an indicator of fault occurrence. The model coefficients and wiring parameters estimation procedure can be obtained as follows:

- First, the model coefficients such as a_2, a_1, a_0, b_1, and b_0 should be estimated using the frequency domain information of circuit voltage and current which are measured within SSPC.
- Then, the wiring parameters such as resistance r, inductance l, shunt capacitance c, and shunt conductance g can be approximated with the information of wire length d and load resistance R_L.

And in theory, the model coefficients can be estimated by Equation (3.8) which is derived from (3.7):

$$\begin{bmatrix} V(j\omega_0) \\ V(j\omega_1) \\ \vdots \\ V(j\omega_N) \end{bmatrix} = \begin{bmatrix} I(j\omega_0)\times(j\omega_0)^2 & I(j\omega_0)\times(j\omega_0) & I(j\omega_0) & -V(j\omega_0)\times(j\omega_0) & -V(j\omega_0) \\ I(j\omega_1)\times(j\omega_1)^2 & I(j\omega_1)\times(j\omega_1) & I(j\omega_1) & -V(j\omega_1)\times(j\omega_1) & -V(j\omega_1) \\ \vdots & \vdots & \vdots & \vdots & \vdots \\ I(j\omega_N)\times(j\omega_N)^2 & I(j\omega_N)\times(j\omega_N) & I(j\omega_N) & -V(j\omega_N)\times(j\omega_N) & -V(j\omega_N) \end{bmatrix} \begin{bmatrix} a_2 \\ a_1 \\ a_0 \\ b_1 \\ b_0 \end{bmatrix} . \quad (3.8)$$

Equations (3.8) can be rewritten with the known voltage vector ***V***, known model vector ***M*** and unknown coefficient vector $\hat{\theta}$ as follows:

$$V = M\hat{\theta}\,. \tag{3.9}$$

In a wide frequency spectrum, different sets of voltage and current equations can be obtained at different frequency points. In Equation (3.8), *N* means that the number of voltages and currents equations such is used for evaluation of model coefficients. This *N* value should be chosen properly to obtain the comprehensive effect of broadband frequency disturbance during fault condition, but it is computationally expensive. With high *N* value, the errors such are associated with the voltage and current sensors can be averaged out or reduced. the Vector $\hat{\theta}$ can be obtained by using the least squares method as follows:

$$\hat{\theta} = \left[M^{\mathrm{T}} M\right]^{-1} M^{\mathrm{T}} V\,. \tag{3.10}$$

According to Equation (3.10), the model coefficients can be estimated by analyzing the electrical signals in frequency domain. After estimating the model coefficients, the wiring parameters, such as shunt capacitance *c*, inductance *l*, shunt conductance *g*, and resistance *r*, can also be solved according to Equations (3.2) to (3.6) as follows:

$$c = \frac{b_1}{R_L d}\,, \tag{3.11}$$

$$l = \frac{a_2}{c R_L d^2}\,, \tag{3.12}$$

$$g = \frac{b_0}{R_L d}, \tag{3.13}$$

$$r = \frac{a_0 - R_L}{d + gR_L d^2}. \tag{3.14}$$

The error e between the present estimated model coefficient/wiring parameter and normal or previously estimated model coefficient/wiring parameter can be expressed as:

$$\mathrm{e} = \left(\frac{\left|\text{normal value - estimated value}\right|^2}{(\text{noramal value})^2} \right). \tag{3.15}$$

According to be above-mentioned approach, the normal inductance l and capacitance c values are estimated along with different number (N) of voltage and current equations as shown in Fig. 3.1 and Fig. 3.2, respectively. The actual inductance and capacitance values are 0.976μH and 31.76pF respectively. When N is equal to 60, the proposed method approximated both inductance and capacitance values with least error. Hence, the N value plays key role for

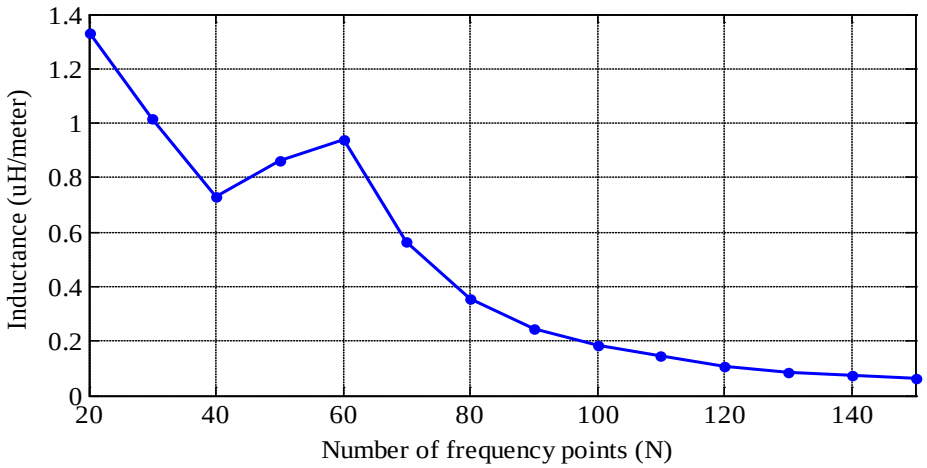

Fig. 3.1 Estimated inductance l (μH/meter) values versus number of frequency points (N)

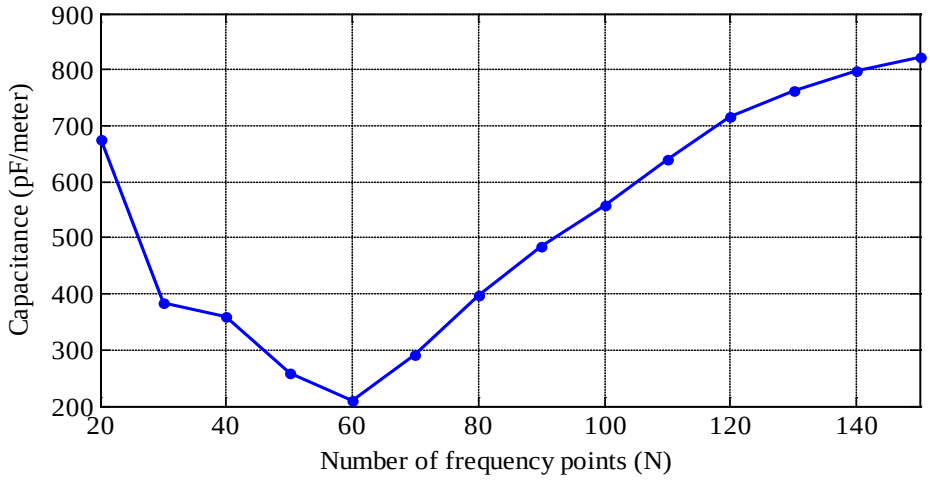

Fig. 3.2 Estimated capacitance *c* (pF/meter) values versus number of frequency points (*N*)

accurate estimation of wiring parameters and model coefficients.

Intermittent arc is quick and disappears in a few (less than 10) milliseconds. Therefore, Equation (3.15) should be evaluated for every pre-determined sampling period to identify the occurrence of intermittent arc faults. Occurrence can be determined when

$$|\mathrm{e}| \geq \delta\,, \tag{3.16}$$

where δ is a predetermined threshold. To make the proposed method suitable for SSPC-based aircraft PDS, the voltage and the current sensors contained in the SSPC should be able to capture the load circuit voltage and current signals in sub-millisecond/sub-microsecond intervals, according to the duration of typical intermittent faults (less than 10 milliseconds).

3.3 GA-Based Fault Location Estimation

The hard wiring faults such as the short-circuit and open-circuit can possibly be detected and located by using TDR when the flight is on the ground. However, intermittent fault phenomenon may not be repeatable when the airplane is back on the ground which makes the intermittent fault location estimation elusive. Intermittent fault may not be hazardous initially, but it would gradually evolve into a serious fault which may cause equipment loss and catastrophic incidents. Hence, a simple yet effective algorithm should be developed for estimation of the intermittent arc location. In this section, the genetic algorithm is introduced to accomplish fault location estimation based on load circuit modeling including intermittent fault and its coefficients.

Starting with the problem formulation, the transfer function of the load circuit including intermittent fault and resistive load can be given as follows according to Equation (2.32):

$$\frac{1}{Z(s)} = \frac{I(s)}{V(s)} = \frac{b_3 s^3 + b_2 s^2 + b_1 s + b_0}{a_4 s^4 + a_3 s^3 + a_2 s^2 + a_1 s + a_0 + 1}, \tag{3.17}$$

The coefficients of Equation (3.17) can be expressed according to Equation (2.32) as follows:

$$a_4 = l^2 c^2 d_1^2 d_2^2, \tag{3.18}$$

$$a_3 = 2rlc^2 d_1^2 d_2^2 + 2gcl^2 d_1^2 d_2^2 + \frac{l^2 c d_1^2 d_2}{R_L} + \frac{l^2 c d_1 d_2^2}{R_L}, \tag{3.19}$$

$$a_2 = \left.\begin{array}{l} lcd_1^2 + lcd_2^2 + lcd_1 d_2 + l^2 g^2 d_1^2 d_2^2 + c^2 r^2 d_1^2 d_2^2 + 4gcrld_1^2 d_2^2 + \dfrac{2rlcd_1^2 d_2}{R_L} \\ + \dfrac{2rlcd_1 d_2^2}{R_{arc}} + \dfrac{l^2 g d_1^2 d_2}{R_L} + \dfrac{l^2 g d_1 d_2^2}{R_{arc}} + \dfrac{l^2 d_1 d_2}{R_L R_{arc}} \end{array}\right\}, \tag{3.20}$$

$$a_1 = \left.\begin{array}{l} lgd_1^2 + lgd_2^2 + crd_1^2 + crd_2^2 + crd_1d_2 + lgd_1d_2 + 2rlg^2d_1^2d_2^2 + 2gcr^2d_1^2d_2^2 + \dfrac{ld_1}{R_{arc}} \\ + \dfrac{ld_1}{R_L} + \dfrac{ld_2}{R_L} + \dfrac{2rlgd_1^2d_2}{R_L} + \dfrac{2rlgd_1d_2^2}{R_{arc}} + \dfrac{cr^2d_1^2d_2}{R_L} + \dfrac{cr^2d_1d_2^2}{R_{arc}} + \dfrac{2rld_1d_2}{R_LR_{arc}} \end{array}\right\}, \quad (3.21)$$

$$a_0 = \left.\begin{array}{l} grd_1^2 + grd_2^2 + r^2g^2d_1^2d_2^2 + rgd_1d_2 + \dfrac{rd_1}{R_{arc}} + \dfrac{rd_2}{R_L} + \dfrac{gr^2d_1^2d_2}{R_L} + \dfrac{gr^2d_1d_2^2}{R_{arc}} \\ + \dfrac{r^2d_1d_2}{R_LR_{arc}} \end{array}\right\}, \quad (3.22)$$

$$b_3 = lc^2d_1d_2^2, \quad (3.23)$$

$$b_2 = rc^2d_1d_2^2 + 2gcld_1d_2^2 + \frac{lcd_1d_2}{R_L} + \frac{l^2cd_2^2}{R_{arc}}, \quad (3.24)$$

$$b_1 = \left.\begin{array}{l} cd_1 + cd_2 + lg^2d_1d_2^2 + 2gcrd_1d_2^2 + \dfrac{lgd_2^2}{R_{arc}} + \dfrac{crd_2^2}{R_{arc}} + \dfrac{ld_2}{R_LR_{arc}} \\ + \dfrac{lgd_1d_2}{R_L} + \dfrac{crd_1d_2}{R_L} \end{array}\right\}, \quad (3.25)$$

$$b_0 = gd_1 + gd_2 + g^2rd_1d_2^2 + \frac{1}{R_L} + \frac{1}{R_{arc}} + \frac{grd_1d_2}{R_L} + \frac{grd_2^2}{R_{arc}} + \frac{rd_2}{R_LR_{arc}}. \quad (3.26)$$

Operating in frequency domain, the Equation (3.17) can be rewritten as follows:

$$I(j\omega_i) = \left.\begin{array}{l} V(j\omega_i)b_3(j\omega_i)^3 + V(j\omega_i)b_2(j\omega_i)^2 + V(j\omega_i)b_1(j\omega_i) + V(j\omega_i)b_0 - I(j\omega_i)a_0 \\ - I(j\omega_i)a_4(j\omega_i)^4 - I(j\omega_i)a_3(j\omega_i)^3 - I(j\omega_i)a_2(j\omega_i)^2 - I(j\omega_i)a_1(j\omega_i) \end{array}\right\}, \quad (3.27)$$

where the definition of $j\omega_i$, $V(j\omega_i)$ and $I(j\omega_i)$ are same as in Section 3.2. Equation (3.27) represents the load system under faulty conditions, in which all the model coefficients a_0,…, a_4

and $b_0,\ldots, b_3$ contain some/all fault-related parameters d_1, d_2 and R_{arc}. Among all model coefficients $a_0,\ldots, a_4$ and $b_0,\ldots, b_3$, only one model coefficient which contain all the fault-related parameters d_1, d_2 and R_{arc}, will be used for the fault parameter identification. This process can be accomplished simply in two steps:

1. First, the faulty model coefficients should be estimated with the response of the load circuit under fault condition.
2. Substitute the estimated model coefficient into its expression for estimation of fault-related parameters.

For estimation of model coefficients, Equation (3.27) should modify in matrix form as follows:

$$\begin{bmatrix} I(j\omega_0) \\ I(j\omega_1) \\ \vdots \\ I(j\omega_N) \end{bmatrix} = \begin{bmatrix} V(j\omega_0)\times(j\omega_0)^3 & \ldots & V(j\omega_0)\times(j\omega_0) & V(j\omega_0) & -I(j\omega_0)\times(j\omega_0)^4 & \ldots & -I(j\omega_0)\times(j\omega_0) & -I(j\omega_0) \\ V(j\omega_1)\times(j\omega_1)^3 & \ldots & V(j\omega_1)\times(j\omega_1) & V(j\omega_1) & -I(j\omega_1)\times(j\omega_1)^4 & \ldots & -I(j\omega_1)\times(j\omega_1) & -I(j\omega_1) \\ \vdots & \vdots & \vdots & \vdots & \vdots & \vdots & \vdots & \vdots \\ V(j\omega_N)\times(j\omega_N)^3 & \ldots & V(j\omega_N)\times(j\omega_N) & V(j\omega_N) & -I(j\omega_N)\times(j\omega_N)^4 & \ldots & -I(j\omega_N)\times(j\omega_N) & -I(j\omega_N) \end{bmatrix} \begin{bmatrix} b_3 \\ \vdots \\ b_0 \\ a_4 \\ \vdots \\ a_0 \end{bmatrix} \tag{3.28}$$

The unknown model coefficients vector in Equation (3.28) can be obtained as follows:

$$\hat{\boldsymbol{\theta}} = \left[\boldsymbol{M}^{\mathrm{T}}\boldsymbol{M}\right]^{-1}\boldsymbol{M}^{\mathrm{T}}\boldsymbol{I}\,. \tag{3.29}$$

In this thesis, b_0 is chosen for the identification of fault parameters for the following four key reasons:

1. The frequency dependent coefficients a_4 to a_1 and b_3 to b_1 are physically very small, which may cause computational problems.

2. There is always some error associated with the estimation of coefficients a_4 to a_1 and b_3 to b_1 because of their small values and influence of N value.
3. The effect of mutual inductance and capacitance must be considered if the wire is located in a bundle which increases the computational burden. Otherwise, larger deviations may occur in the fault location estimation.
4. The coefficient a_0 is small and contains many variables compared with b_0, which would affect the convergence speed and the accuracy of the identification algorithm.

First b_0 (or $b_{0,\,est}$) should be estimated according to Equations (3.28) and (3.29), using frequency domain information of the circuit voltage and current recorded by SSPC. Then a fitness function with its expression $b_{0,\,\exp}$ is given as follows:

$$f(d_1, R_{arc}) = \frac{\left| b_{0,est} - b_{0,\exp} \right|^2}{b_{0,est}{}^2}, \tag{3.30}$$

which does not contain d_2 because when wire length d is known, d_2 can be easily obtained by:

$$d_2 = d - d_1. \tag{3.31}$$

Furthermore, the fitness function should be minimized by using an efficient optimization technique for the estimation of fault parameters as follows:

$$\text{minimize } f(d_1, R_{arc}). \tag{3.32}$$

The wire resistance r/meter, shunt conductance g/meter, wire length d and load information R_{L} should be known or estimated prior to minimizing the fitness function. The wire resistance

and conductance can be approximated according to Equations (3.13) and (3.14) under particular or normal working conditions. If the load is resistive, its resistance R_L can be approximated using the preceding or fast sampling period information as follows:

$$R_L = \frac{a_0 - rd}{1 + rgd^2} \tag{3.33}$$

In the above equation, the wire resistance r and conductance g are frequency independent. Once their values are known, they can be utilized continuously for the approximation of resistive load resistance along with known d value.

3.3.1 Genetic Algorithm

Genetic algorithms (GAs) are one of most widely-used global search and optimization methods and they are developed with the motivation of natural biological evolution [34]. A genetic algorithm is proposed to solve the optimization problem as given in Equation (3.31) because of following:

- It does not require any derivatives for searching as does the gradient method used in [35];
- There is no need of providing starting point or initial guess. In other words, GA itself selects the starting points or initial guess of estimates.
- It is computationally simple;
- It can converge quickly with good estimates [34].

GA maintains a population of individual estimates and each estimate can be represented by a specific symbol x_1 or x_2 or other. It then selects the feasible population randomly from a given space. This space can also be called a search space. GA can be restricted to search in a certain space by using the lower and upper boundaries, which improves the quality of the search and speed of convergence. The prior knowledge about estimates must be known to set the boundary limits. For example, if the wire length d is 20 meters, the fault can possibly occur between 0 and 20 meters. Hence, the lower and upper boundary limits for d_1 can be set to 0 and 20 meters, respectively. Intermittent arc fault resistance R_{arc} is unknown and cannot be predictable. Therefore, lower and upper boundary limits for R_{arc} can be set to 0 and infinity ohms, respectively.

GA is not a directionless method; it utilizes the knowledge from the previous set of estimates in order to generate new estimates, which would minimize the fitness function with the use of genetic operations such as *crossover* and *mutation* [34,36]. GA is probabilistic in nature, not deterministic [34]. GA essentially works in parallel. As one of the potential features of GA, this enables it to deal with the numerous solutions simultaneously. However, this parallel evaluation has more memory requirements than others.

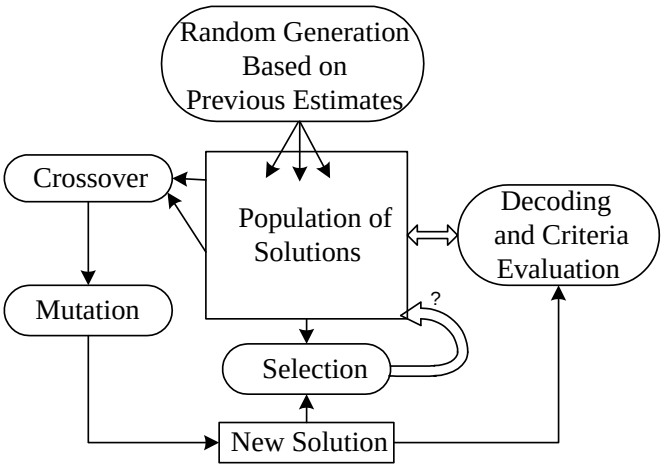

Fig. 3.3 Structure of a steady-state GA [34]

A steady-state GA is shown in Fig. 3.3. Initially, GA produces population (or parents) of estimates randomly. The genetic operator, *crossover*, selects the two parents with a probability P_c proportional to their fitness values and then it produces an offspring (or child) from the selected two-parent solutions which mimics the natural biological evolution. Another genetic operator is *mutation*, would receive the output of the crossover operator with a probability of P_m. Every new solution is decoded to estimate the fitness function values. The fitness scaling function scales the individuals with highest fitness value that is suitable for the selection function. The selection function identifies the good solutions which will join in the population, while the worst solutions would be removed from the population. This total process will be continued until the given termination condition is met.

The iterative process occurs as:

$$\left.\begin{array}{l} f\left(d_1, R_{arc}\right) \neq K \\ \vdots \\ f\left(d_1, R_{arc}\right) = K \end{array}\right\}, \tag{3.34}$$

where K is a predetermined fitness limit value. GA continuously updates the fitness function with different fault parameters and it stops the optimization when the given condition is met, generating estimates of the location of fault and its resistance. GA does not minimize the fitness function if $b_{0,\ est}$ is obtained from normal data, including switching variations and/or load transients.

3.4 Summary

This chapter addressed the effective methods for estimation of normal model coefficients and wiring parameters, and intermittent arc fault detection. Intermittent arc fault causes the broadband frequency disturbance in voltage and current. Hence, the proposed methods are derived in the frequency domain. An efficient mathematical Equation (3.16) is developed to identify the occurrence of intermittent fault. Furthermore, a fitness function is formulated to estimate the fault-related parameters such as intermittent arc location and average fault resistance based on a faulty load circuit model coefficient b_0. Finally, a genetic algorithm (GA) is proposed to minimize the formulated fitness function.

CHAPTER 4

SIMULATION AND EXPERIMENTAL RESULTS

4.1 Overview

This chapter consists of five sections. The first section provides an overview. In the second section, simulations will be performed on the load circuit which were comprised of 20 meters wire and resistive loads (R=15 ohms), under three different operating conditions, such as turning-on of load circuit, normal and fault conditions. The details about the experimental setup are given in the third section. The fourth section presents the experimental results on model coefficients and wiring parameters estimation of a typical load circuit, intermittent arc fault detection and location. The load circuit includes 16 AWG (American wire gauge) power wire and a resistive load (R=53 ohms), and the length d of wire is 24.6 meters. The proposed methods will be verified under five different conditions, such as turn-on of load circuit, normal condition, fault condition 1, fault condition 2 and turn-off of load circuit, which commonly occur in a dynamic aircraft PDS. The fifth section is a summary of the chapter.

4.2 Simulation Results

In this section, feasibility of the proposed methods is verified by simulations using MATLAB/Simulink. The parameters of the simulation model are provided in Table 4.1. The model of simulation is shown in Fig. 4.1 and comprises a fixed 3 phase AC voltage source, 12 pulse diode rectifier, load circuit including 20 meter wire and resistive load (15 ohms), and intermittent arc fault model. The load circuit is powered by 28V DC supply and it is obtained

from constant AC voltage source (115V, 400 Hz) through AC/DC 12-pulse diode rectifier and LC filter.

TABLE 4.1 SIMULATION PARAMETERS

Parameter	Description	Value
V	Input voltage (DC)	28 V
d	Wire length	20 m
d_1	Distance to fault	14 m
R_L	Load resistance	15 Ω
r	Wire resistance/m	0.046 Ω
l	Wire inductance/m	0.976 µH
c	Wire shunt capacitance/m	31.76 pF
g	Wire shunt conductance/m	0.97 µS
f_s	Sampling frequency	250 kHz

V = volt, m = meter, H = Henry, F= faraday, S = Siemens

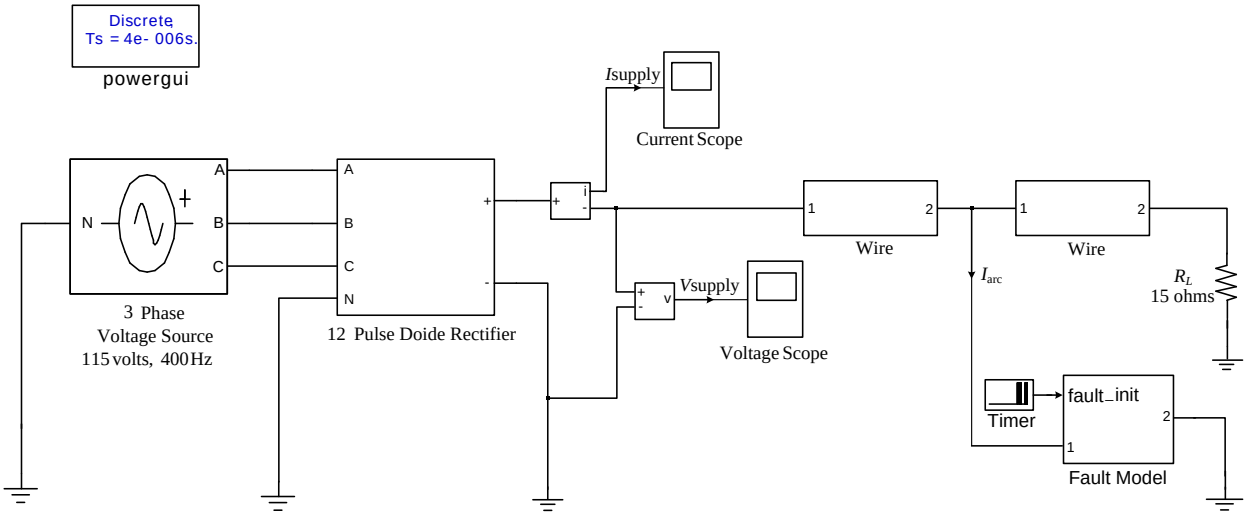

Fig. 4.1 Model of simulation

The simulation of a line-to-ground intermittent arc is difficult. This is obtained by modeling the non-linear arc resistance R_{arc} as a $6.8\times e^{-(0.001375\times i_{arc})}$ and with use of timer. The wire is modeled with the resistance, inductance, shunt capacitance and shunt conductance, as shown in Fig. 2.4. The distance d_1 to the fault is 14 meters. The load circuit supply voltage V_{supply} and supply current I_{supply} are shown in Fig.4.2. The curves in Fig. 4.2 show the scenario that voltage drops to a certain value due to an intermittent arc fault, and, then, it gradually recovers back to its actual value. These voltage and current samples are divided into three cases such as a switching event (first 1024 data points of voltage and current), normal (1025 to 2048 data points) and fault (2049 to 3072) data points for fault examination.

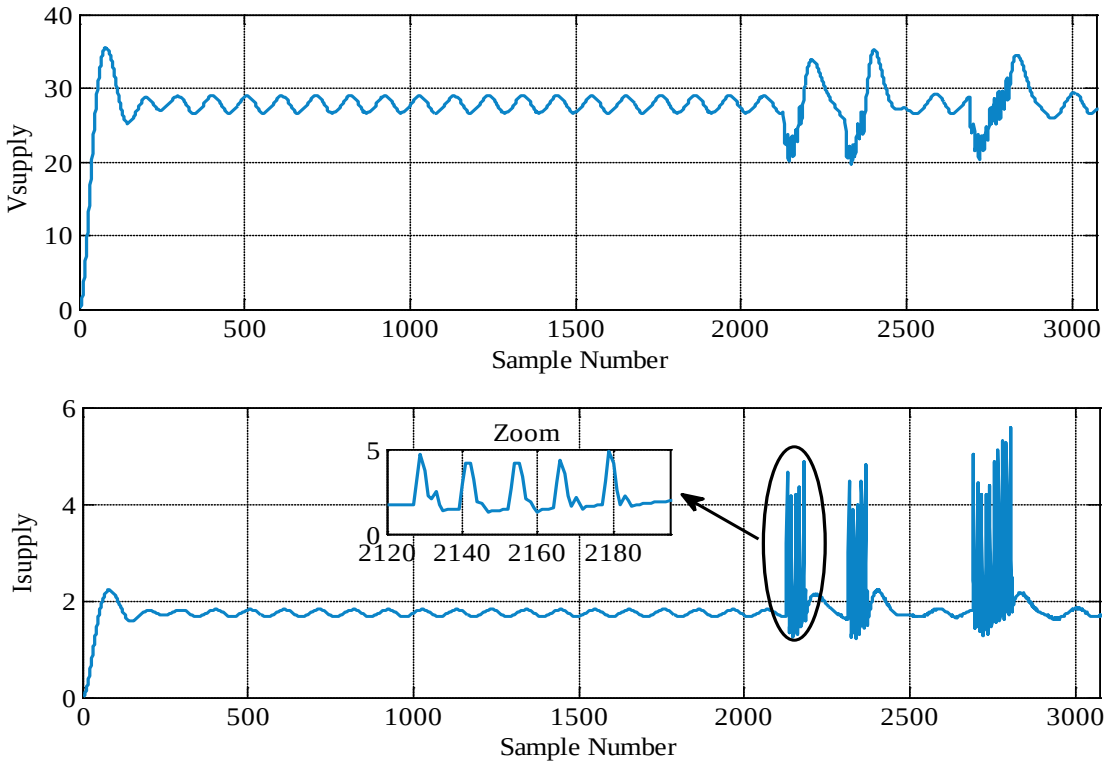

Fig. 4.2 Load circuit supply voltage and current waveform

MATLAB cannot inverse the model vector ***M*** if it is close to singular or not square. To compute this, the Moore-Penrose pseudo-inverse method is used in this thesis. However, this method may be inefficient if inverse operation has multiple solutions. Such a situation can occur while evaluating the frequency independent coefficients a_0 and b_0 of Equation (3.10). To resolve this problem, GA is used to estimate the frequency independent coefficients of Equation (3.10) by solving the following:

$$\text{minimize } f(a_0, b_0), \tag{4.1}$$

where,

$$f(a_0, b_0) = V(j\omega_0) - (I(j\omega_0) \times a_0) - (V(j\omega_0) \times b_0). \tag{4.2}$$

The following steps are taken once a simulation is executed:

1. Conversion of time domain voltage and current samples into frequency domain using Fast Fourier Transform (FFT) technique;
2. Estimation of model coefficients a_2 a_1, a_0, b_0 and b_1 using Equations (3.8), (3.10) and (4.2);
3. Estimation of wiring parameters *r, l, c* and *g* by using Equations (3.11), (3.12), (3.13) and (3.14);
4. Repeat the steps 1 to 3 for three cases such as the switching event (or turn-on), normal condition and fault condition;
5. Analyze the estimated model coefficients and wiring parameters under three cases, and evaluate the error *e* value to identify the occurrence of fault.

According to the above-mentioned steps 1 to 4, the model coefficients and wiring parameters are estimated, which are given in Table 4.2 to Table 4.5. In this process, the effect of N value on frequency dependent coefficients a_2, a_1 and b_1 and wiring parameters c and l can be observed. The coefficients a_0 and b_0 and wiring parameters r and g do not depend on N value; they are given in Table 4.2.

Table 4.2 Estimated model coefficients and wiring parameters with N=20

Model coefficients and wiring parameters	N=20		
	Switching event	Normal	Fault
a_2 ($\times 10^{-12}$)	1.813	5.392	575.488
a_1 ($\times 10^{-6}$)	5.547	3.289	15.021
a_0	15.9441	15.9389	14.3586
b_1 ($\times 10^{-6}$)	0.346	0.203	0.4456
b_0	0.011982	0.0012	0.00214
c (pF/m)	1152.9	675.48	1485.2
l ($\mu H/m$)	0.262	1.33	64.58
r (Ω/m)	0.046843	0.04689	N/D
g (μS/m)	3.994291	4.00309	7.1541

Table 4.3 Estimated model coefficients and wiring parameters with N=40

Model coefficients and wiring parameters	N=40		
	Switching event	Normal	Fault
a_2 ($\times 10^{-12}$)	0.244	1.661	120.882
a_1 ($\times 10^{-6}$)	7.0549	1.6634	7.9822
b_1 ($\times 10^{-6}$)	0.4429	0.1074	0.4924
c (pF/m)	1476.22	357.987	1641.64
l ($\mu H/m$)	0.02753	0.73158	12.266

Table 4.4 Estimated model coefficients and wiring parameters with N=60

Model coefficients and wiring parameters	N=60		
	Switching event	Normal	Fault
a_2 ($\times 10^{-12}$)	0.202	1.179	54.377
a_1 ($\times 10^{-6}$)	7.298	0.914	5.6487
b_1 ($\times 10^{-6}$)	0.4584	0.0627	0.4964
c (pF/m)	1528.1	209.14	1654.8
l ($\mu H/m$)	0.022	0.94	5.48

Table 4.5 Estimated model coefficients and wiring parameters with N=80

Model coefficients and wiring parameters	N=80		
	Switching event	Normal	Fault
a_2 ($\times 10^{-12}$)	0.167	0.844	2195.33
a_1 ($\times 10^{-6}$)	7.334	1.808	368.596
b_1 ($\times 10^{-6}$)	0.461	0.118	101.081
c (pF/m)	1535.8	396.64	336935.4
l ($\mu H/m$)	0.018	0.354	1.086

The following points can be summarized based on the values in Table 4.2 to 4.5:

- During normal conditions, the proposed method (N=60) estimated the capacitance c and inductance l values with minimum error of 0.00136 and 31.19 receptively;
- During normal and switching conditions, the proposed method successfully approximated the resistance r and conductance g values with least error of 0.000374 and 9.758 receptively;
- The deviations in frequency-dependent model coefficients a_2, a_1, and b_1 and wiring parameters c and l are in the expected range during the switching event;
- The deviations in model coefficients a_2, a_1, and b_1 are high during fault with all N values because of the broadband frequency disturbance;
- The resistance r is not definable (N/D) with fault data because the estimated a_0 is less than R_L;
- The capacitance c (N=80) and conductance g are deviated to a great extent under fault condition because of the parallel intermittent arc fault;
- The deviations in model coefficients or capacitance are noticeable when N is equal to 80. Hence, N plays a key role in fault detection and thus, the model coefficients and wiring parameters should evaluate with all possible N values.

According to step 5, the error e values (N=80) during case 1 (normal vs. turn-on) and case 2 (normal vs. fault) are evaluated. The results are given in Table 4.6, in which error is high as expected during the fault, case 2.

Table 4.6 Estimated error e values (N=80)

error e of	Case 1	Case 2
a_2	0.643	6.76×10^{6}
a_1	9.342	41.156×10^{3}
b_1	8.449	0.7321×10^{6}
c	8.25	0.72×10^{6}
g	4.8314×10^{-6}	2.4803

Based on error e values of case 2, deviations in the model coefficients and wiring parameters, and the N/D of wire resistance r, the intermittent arc fault can be noticed from normal load circuit switching variations.

By using Equations (3.28) and (3.29), the coefficient $b_{0,\,\mathrm{est}}$ under three cases such as turn-on, normal and fault, is estimated at 0.06254, 0.06256 and 0.06945 respectively. The following steps are carried out once the coefficient $b_{0,\,\mathrm{est}}$ is estimated:

- Clear representation of fitness function with a string of symbols;
- Set the lower and upper boundaries for estimates such as intermittent arc fault location d_1 and its average resistance R_{arc};
- Selection of GA parameters such as population size, crossover probability P_{c}, mutation probability P_{m} and selection procedure;
- Set the GA termination procedure, i.e., fitness limit K value;
- Plot the results.

The GA parameters are given in Table 4.7. The value of fitness limit K is chosen as a 1×10^{-9}. The lower and upper boundaries for the fault location d_1 are set to 0 and 20 meters, respectively. For R_{arc}, the lower and upper boundaries are set to 0 ohms and 1000 ohms, respectively. The estimated r and g values (normal) that are given in Table 4.2 are used for fitness function minimization instead of their original values.

Table 4.7 GA parameters

GA parameters	Population size	Tournament size	P_c
Its value	80	80	0.5

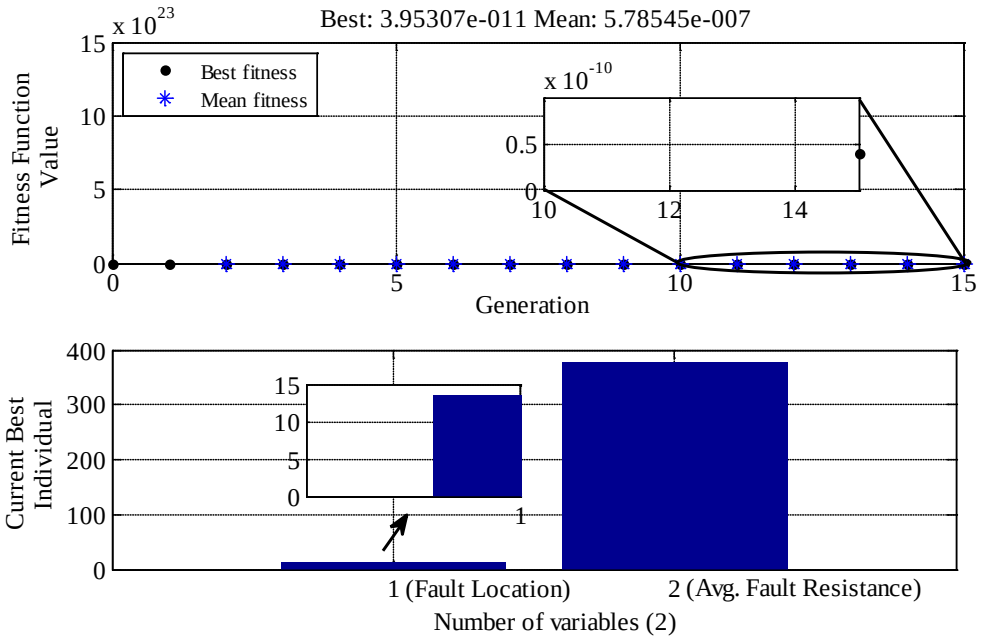

Fig. 4.3 GA results for fault condition (actual d_1 is 14 meters)

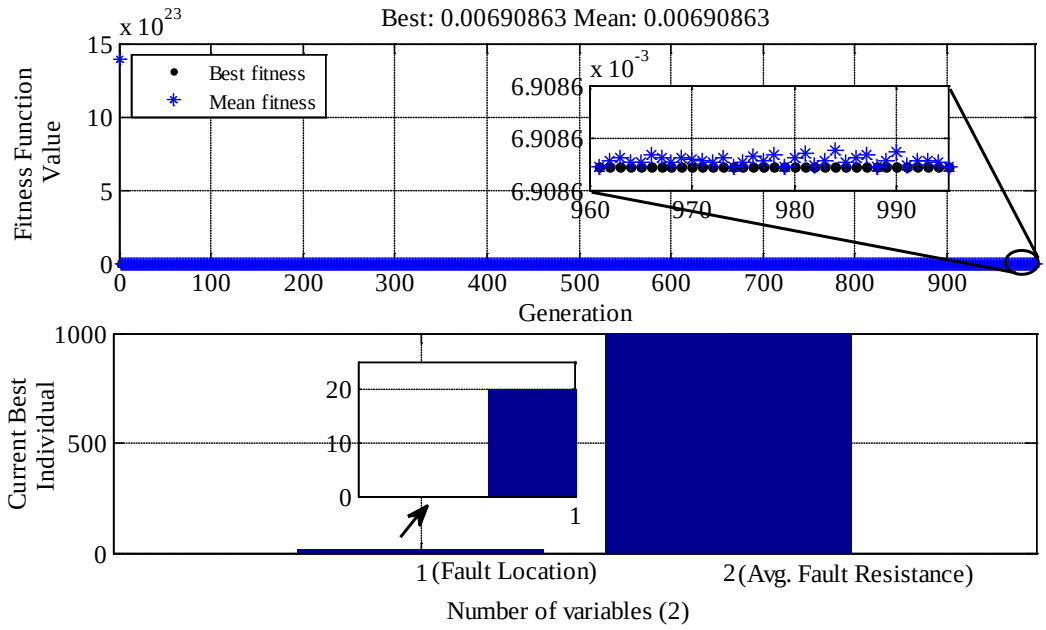

Fig. 4.4 GA results for turn-on condition

The crossover probability (P_c) is one of the most important GA parameters and it combines two past estimates to form a new estimate for next generation or iteration. GA maintains a certain size of population (or estimates) for every generation or iteration. More population leads to better estimation but this affects the convergence speed. Unfortunately, there is no standard/mathematical approach to select GA parameters, and they are often selected based on trial and error.

At this parameter's setting, the proposed GA method successfully estimated the intermittent arc fault location with an accuracy of +/- 0.5 meters on 20 meter wire as shown in Fig. 4.3. The variable non-linear arc fault resistance R_{arc} is adopted to represent the inconsistent arc current I_{arc} during intermittent fault incidence. In Fig. 4.3, the estimate of R_{arc} represents the average value of the constantly changing variable. GA takes 15 generations or iterations to minimize fitness function under fault conditions. As mentioned in the previous section, GA does not minimize the

fitness function under turn-on conditions as shown in Fig. 4.4. GA terminated the optimization procedure after 995 generations, and produced d_1 and R_{arc} as 20 meters and 1000 ohms, respectively, which are the upper boundary limits of fault location and resistance. Hence, it is possible to identify the intermittent arc fault from normal aircraft PDS switching variations.

4.3. Experimental Setup

Fig. 4.5 shows the block diagram of the experimental setup, which includes an adjustable DC power supply, thermal circuit breaker, digital storage oscilloscope (DSO), current amplifier (CA), current and voltage probes, 24.6 meter 16 AWG wire, and resistive load. The load is energized by 28V DC power supply. The adjustable DC power source itself has a protection system and the thermal circuit breaker is also connected for additional protection.

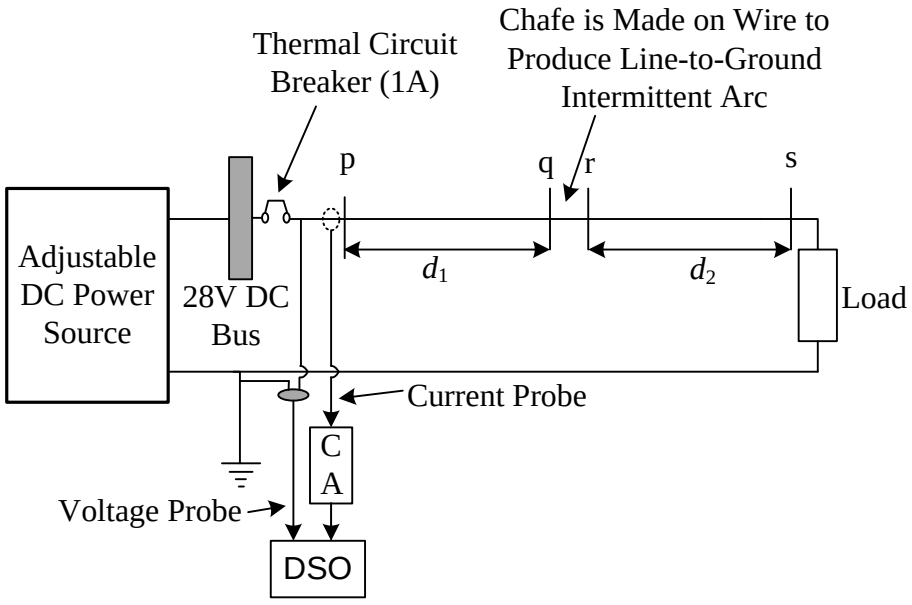

Fig. 4.5 Block diagram of experimental setup

Fig. 4.6 Picture of adjustable DC power supply

The picture of the adjustable DC power supply is given in Fig. 4.6. It operates in two different modes, such as the constant voltage mode and the constant current mode. It produces rated voltage and load-demanded current in constant voltage mode and vice versa. The constant voltage mode is used in this thesis. The power converter can lose its control capability of maintaining of constant voltage during intermittent arc fault conditions due to unbalanced power flow at the input/output. Before turn-on, the “START” button, the rated voltage and current values must be set using “V/I division” button, and voltage and current knobs. If a load change causes the current limit to be exceeded than the predetermined set value, the power supply will automatically crossover to constant current output. But, if a fault causes the current limit to be exceeded, the power supply loses its control capability due to unbalanced power flow at the input/output and it may not be changed into constant current mode. The over current and/or under voltage protection associated in power supply can detect the fault if it stays for enough time period (about a few seconds).

Every test starts with a healthy wire, with no chafes, and later, a chafe fault would be introduced on wire insulation by using a sharp material. Now, the wire insulation is damaged and shows the wire conductor partially. During the tests, a dry line-to-ground intermittent arc fault is simulated by vibrating the chafed wire against the ground which mimics the aircraft environment. The protective devices do not trip the load circuit because the intermittent arc disappears in a few milliseconds before they respond. The voltage and current of the load circuit are measured with a voltage probe and A6303 current probe respectively. The TPS2024 digital storage oscilloscope is used to store voltage and current signals; the DSO acts as a data acquisition system. The current probe is connected to DSO through AM503B current amplifier. The voltage and current signals are measured with a sampling frequency of 250 kHz.

4.4.Experimental Results

In this section, feasibility of the proposed methods is verified by experiments under five different conditions such as turn-on of load circuit, normal, fault 1, fault 2 and turn-off of load circuit. The load circuit input voltage and current signals under normal working conditions are shown in Fig. 4.7. The 250 sampling numbers would be equal to a one millisecond time period. The load circuit voltage and current signals under turn-on and turn-off conditions are initially measured at a sampling frequency of 5 kHz and are re-sampled at a sampling frequency of 250 kHz using the interpolation method in MATLAB. As shown in Fig. 4.8, the upper (or top) voltage waveform is the input to the interpolation method and the bottom voltage waveform is the output of interpolation method. It successfully re-sampled the voltage and current signals by adding new sample values between the two fast sample values. The interpolation method may not alter the structure and basic properties of voltage and current signals.

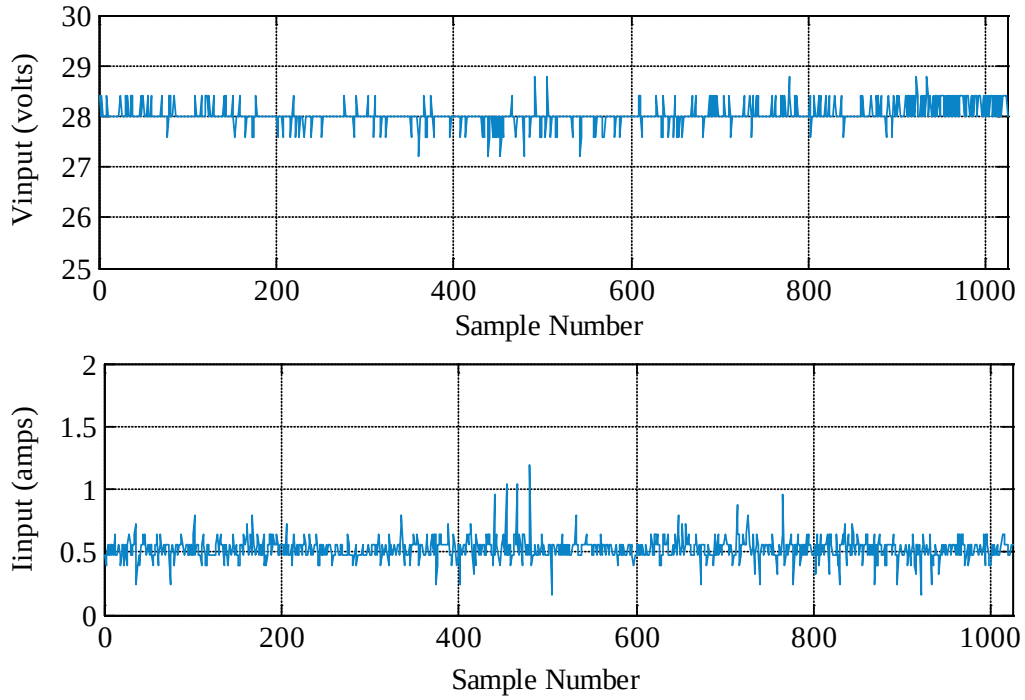

Fig. 4.7 Input voltage and current of load circuit under normal condition

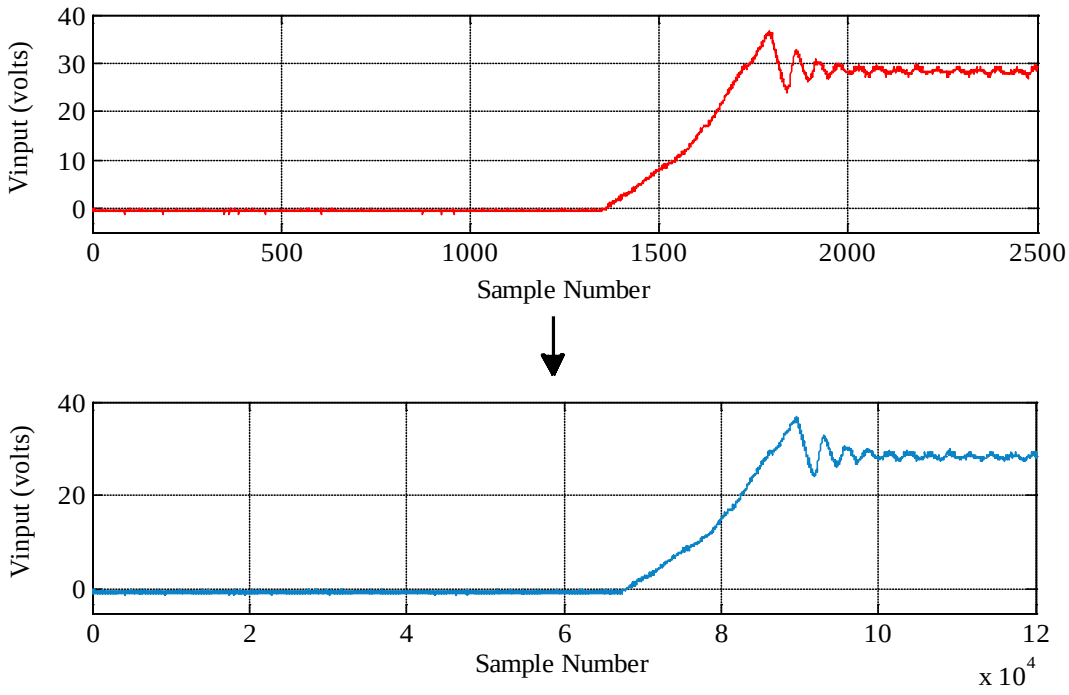

Fig. 4.8 Load circuit turn-on voltage waveform before (top) and after (bottom) interpolation method

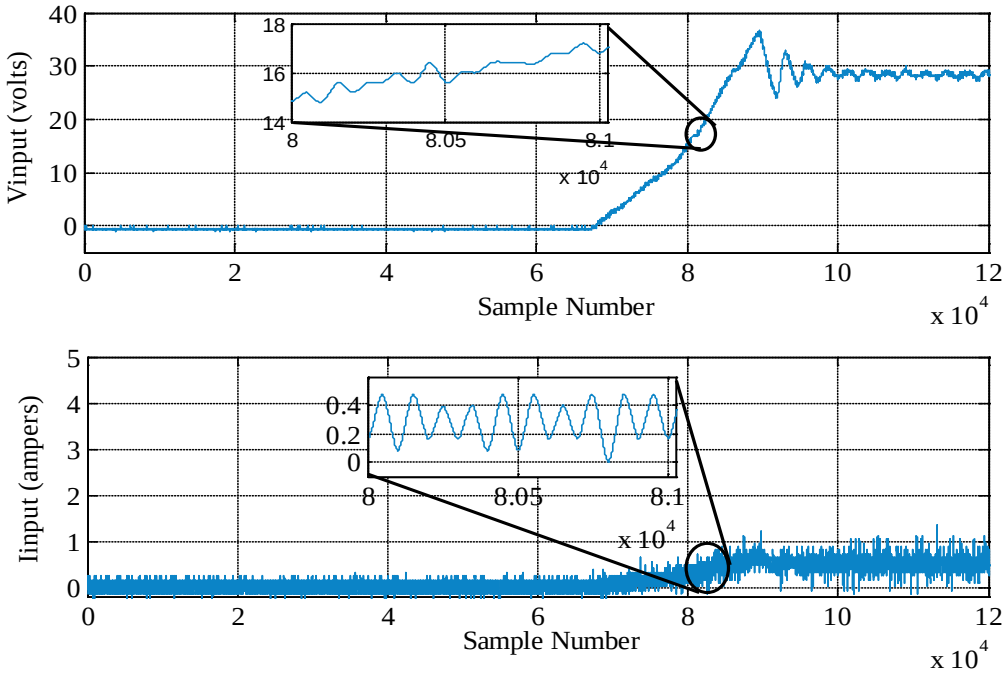

Fig. 4.9 Input voltage and current of load circuit under turn-on condition

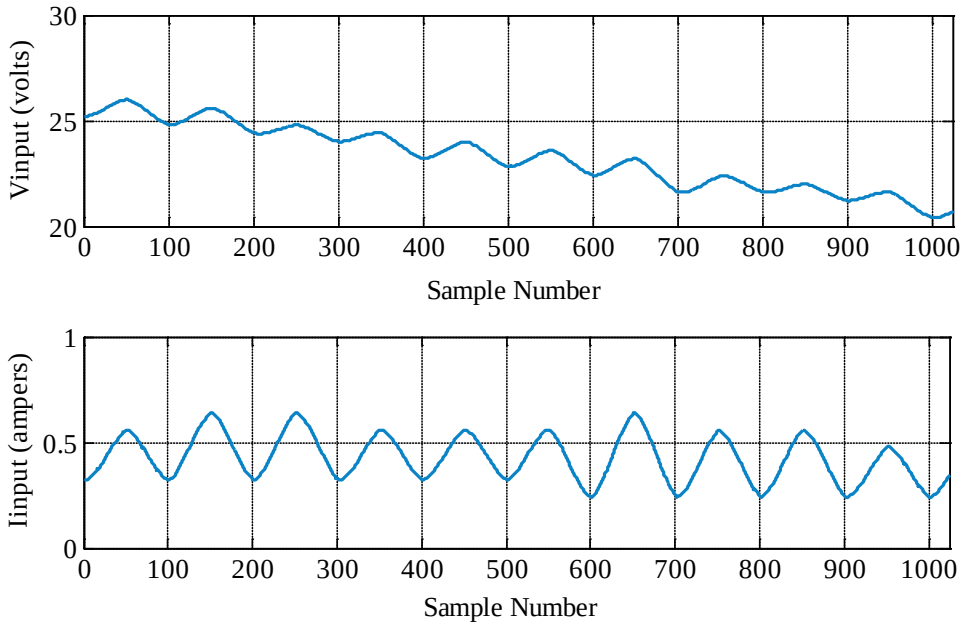

Fig. 4.10 Input voltage and current of load circuit under turn-off condition

The input voltage and current of the load circuit under turn-on conditions is shown in Fig. 4.9 as are output results of interpolation. Among these samples, only 1024 voltage and current samples are used for fault examination, which are shown in zoom. The load circuit input voltage and current signals under turn-off conditions are shown in Fig. 4.10, where the 250 sampling numbers would be equal to a one millisecond time period.

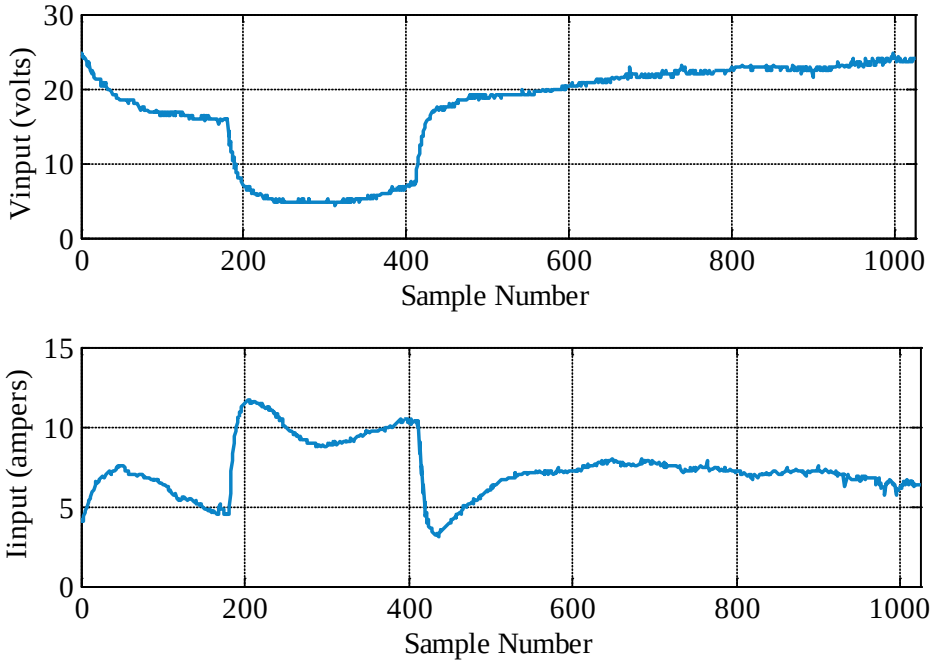

Fig. 4.11 Input voltage and current of load circuit under fault condition 1

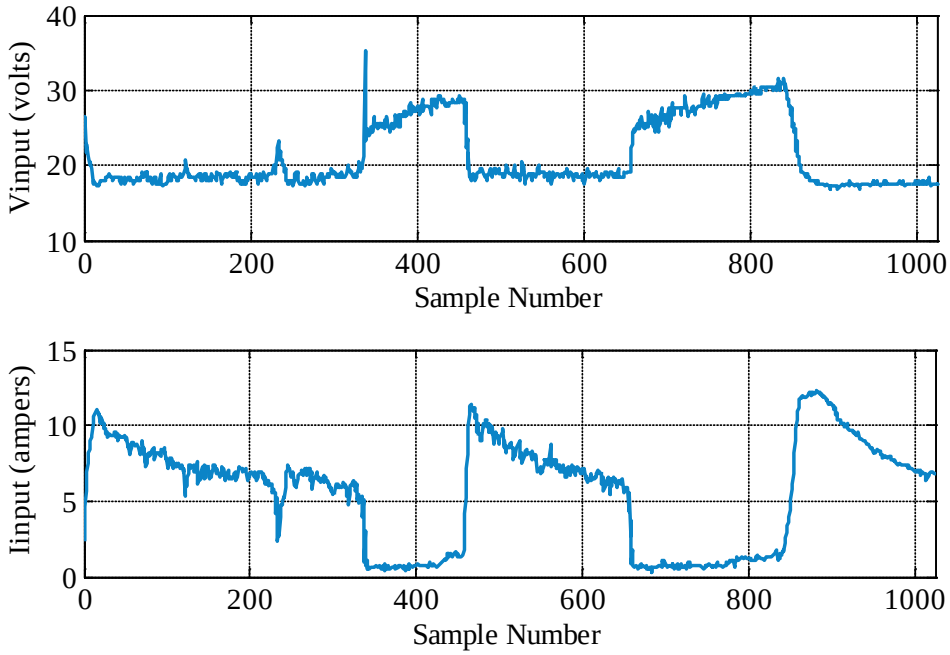

Fig. 4.12 Input voltage and current of load circuit under fault condition 2

The load circuit input voltage and current under fault condition 1 and fault condition 2 are shown in Fig. 4.11 and Fig. 4.12, respectively. The curves in Figs. 4.11 and 4.12 depict the scenario that voltage drops to a certain value due to an intermittent arc fault, and, then, it gradually recovers back to its actual value. The distance d_1 to the fault is 19.8 meters under fault condition 1 which is close to load, and the d_1 is 4.8 meters under fault condition 2 which is near the power bus. The 250 sampling numbers would be equal to one millisecond time period which means that the intermittent arc only lasts a few (less than 10) milliseconds.

After collecting the voltage and current samples from DSO, the following steps are taken to analyze the fault:

1. By using FFT method, the time domain voltage and current signals are converted into frequency domain;

2. Estimation of model coefficients a_2 a_1, a_0, b_0 and b_1 using Equations (3.8), (3.10) and (4.2);
3. Estimation of wiring parameters *r*, *l*, *c* and *g* by using Equations (3.11), (3.12), (3.13) and (3.14), and information of load resistance *R* value and wire length *d*;
4. Repeat steps 1 to 3 for all five cases, turn-on, normal condition, fault condition 1, fault condition 2 and turn-off;
5. Calculate error *e* value based on the estimated model coefficients and wiring parameters to recognize the intermittent arc fault incident.

According to the above-mentioned steps 1 to 4, the model coefficients and wiring parameters are estimated which are given in Table 4.8 to Table 4.11, where, the effect of *N* value on the frequency dependent coefficients a_2, a_1 and b_1, and wiring parameters *c* and *g* can be noticed. The other coefficients a_0 and b_0, and parameters *r* and *g* are given under the column of *N*=80 which does not mean that they depend on *N*. As mentioned earlier, the deviations in model coefficients during two fault conditions are obvious because the broadband frequency disturbance and the resistance *r* is not definable (N/D) under fault conditions since the estimated a_0 is less than R_L. Furthermore, the shunt wire parameters, such as *c* and *g*, are affected to a great extent under fault conditions because of parallel intermittent arc fault. The estimated inductance value *l* does not seem feasible under turn-off conditions. As the derived Equation (3.12) for inductance estimation is not unique, Equation (3.12) also depends on estimated capacitance value, and the inconsistent distance between the positive wire and the ground may result in slight deviations in capacitances and inductances. One thing can be clearly observed from these tables – the wire with high capacitance has low inductance and vice versa.

Table 4.8 Estimated model coefficients and wiring parameters with N=80 (Experimental)

Model coefficients and wiring parameters	N=80				
	Turn-on	Normal	Fault cond. 1	Fault cond. 2	Turn-off
a_2 ($\times 10^{-12}$)	4.416	3.365	692.686	890.24	20.572
a_1 ($\times 10^{-6}$)	1.222	0.522	49.541	61.22	1.456
a_0	56.65	53.353	2.6996	4.2241	55.29
b_1 ($\times 10^{-6}$)	0.0695	0.0503	106.566	8.22	0.0134
b_0	0.01364	0.00465	0.15899	0.1292	0.0136
c (pF/m)	53.354	38.58	81735.1	6302.9	10.334
l ($\mu H/m$)	2.581	2.72	0.2642	4.403	62.063
r (Ω/m)	0.14646	0.01429	N/D	N/D	0.0918
g (µS/m)	10.466	3.56726	121.95	99.114	10.466

Table 4.9 Estimated model coefficients and wiring parameters with N=100 (Experimental)

Model coefficients and wiring parameters	N=100				
	Turn-on	Normal	Fault cond. 1	Fault cond. 2	Turn-off
a_2 ($\times 10^{-12}$)	3.559	0.875	473.393	3340.435	30.585
a_1 ($\times 10^{-6}$)	1.211	0.241	44.156	314.631	1.5364
b_1 ($\times 10^{-6}$)	0.07383	0.02447	137.674	47.4366	0.01022
c (pF/m)	56.626	18.7685	105594.7	36383.362	7.83493
l ($\mu H/m$)	1.9597	1.4528	0.13977	2.8626	121.71

Table 4.10 Estimated model coefficients and wiring parameters with N=180 (Experimental)

Model coefficients and wiring parameters	N=180				
	Turn-on	Normal	Fault cond. 1	Fault cond. 2	Turn-off
a_2 ($\times 10^{-12}$)	1.293	0.436	2807.2	993.04	13.646
a_1 ($\times 10^{-6}$)	1.207	0.172	630.81	218.95	1.3437
b_1 ($\times 10^{-6}$)	0.0739	0.0061	1083.4	15.852	0.0125
c (pF/m)	56.72	4.693	830921	12158	9.657
l ($\mu H/m$)	0.711	2.896	0.1053	2.54	44.054

Table 4.11 Estimated model coefficients and wiring parameters with N=200 (Experimental)

Model coefficients and wiring parameters	N=200				
	Turn-on	Normal	Fault cond. 1	Fault cond. 2	Turn-off
a_2 ($\times 10^{-12}$)	1.022	0.492	2275.16	772.118	16.222
a_1 ($\times 10^{-6}$)	1.2057	0.2034	356.658	196.88	1.3008
b_1 ($\times 10^{-6}$)	0.0751	0.00373	506.079	20.211	0.0171
c (pF/m)	57.622	2.8588	388157.1	15501.73	13.112
l ($\mu H/m$)	0.55303	5.3663	0.18275	1.55295	38.5722

The estimated error e value during case 1 (normal vs. turn-on), case 2 (normal vs. turn-off), case 3 (normal vs. fault 1) and case 4 (normal vs. fault 2) are given in Table 4.12, in which the error is very obvious as expected during fault conditions i.e., case 3 and case 4. Therefore, the intermittent arc fault can be distinguished from normal load circuit switching variations based on deviations in model coefficients and wiring parameters, including the error e and the N/D of wire resistance r.

Table 4.12 Estimated error *e* values during four cases (*N*=180)

error *e* of	Case 1	Case 2	Case 3	Case 4
a_2	3.863	918	41.4×10^{6}	5.18×10^{6}
a_1	36.21	46.4	13.44×10^{6}	1.62×10^{6}
b_1	123.53	1.1	3.15×10^{10}	6.74×10^{6}
c	122.9	1.1188	3.13×10^{10}	6.71×10^{6}
g	3.73	3.73	1101.3	717.4

The estimated coefficient $b_{0,\,est}$ values are given in table 4.13. Its value remains the same under normal conditions including turn-on and turn-off, and altered under fault conditions. The important crossover probability P_c is selected as 0.5, the size of population and tournament are selected as 80, and the value of the fitness limit K is chosen as 1×10^{-7}. Most of the GA parameters are the same during the simulations and experiments, except the K value and boundaries of estimates or fault parameters. The lower and upper boundaries for the intermittent arc location d_1 are set to 0 meters and 24.6 meters, respectively. Intermittent arc occurs in unpredictable manners and thus, the intermittent arc resistance is unknown. So, the lower and

Table 4.13 Estimated coefficient $b_{0,\,est}$ values under five conditions

Condition	$b_{0,\,est}$ value
Turn-on	0.0178
Turn-off	0.0183
Normal	0.0188
Fault condition#1	0.362
Fault condition#2	0.249

upper boundaries for the average fault resistance R_{arc} are set to 0 ohms and infinity ohms, respectively.

GA parameters are selected based on trial and error. At this parameters setting, the proposed GA successfully estimated the location of two different intermittent arcs with an accuracy of +/- 0.5 meters on 24.6 meter wire as shown in Fig. 4.13 and Fig. 4.14, in which, the estimate of R_{arc} represents the average value of the constantly changing variable. GA takes approximately 100 generations to minimize fitness function under two fault conditions.

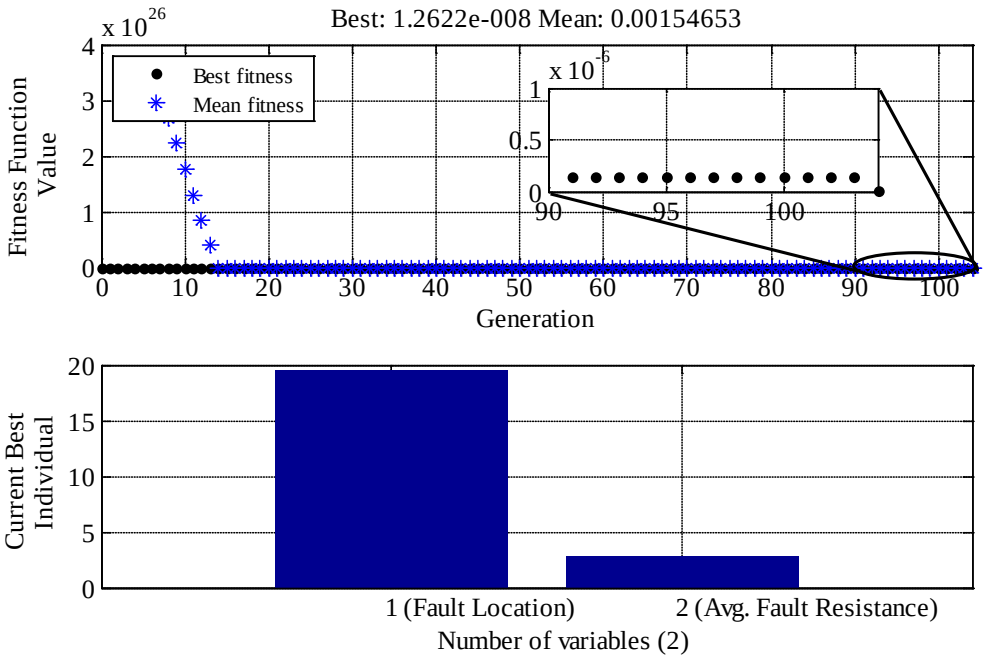

Fig. 4.13 GA results for fault condition 1 (actual d_1 is 19.8 meters)

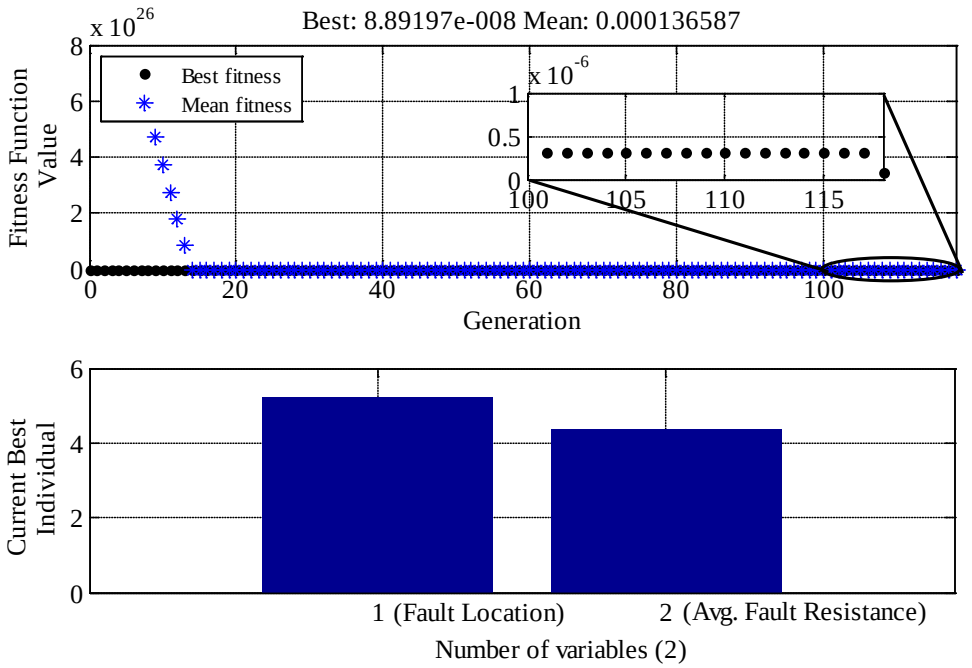

Fig. 4.14 GA results for fault condition 2 (actual d_1 is 4.8 meters)

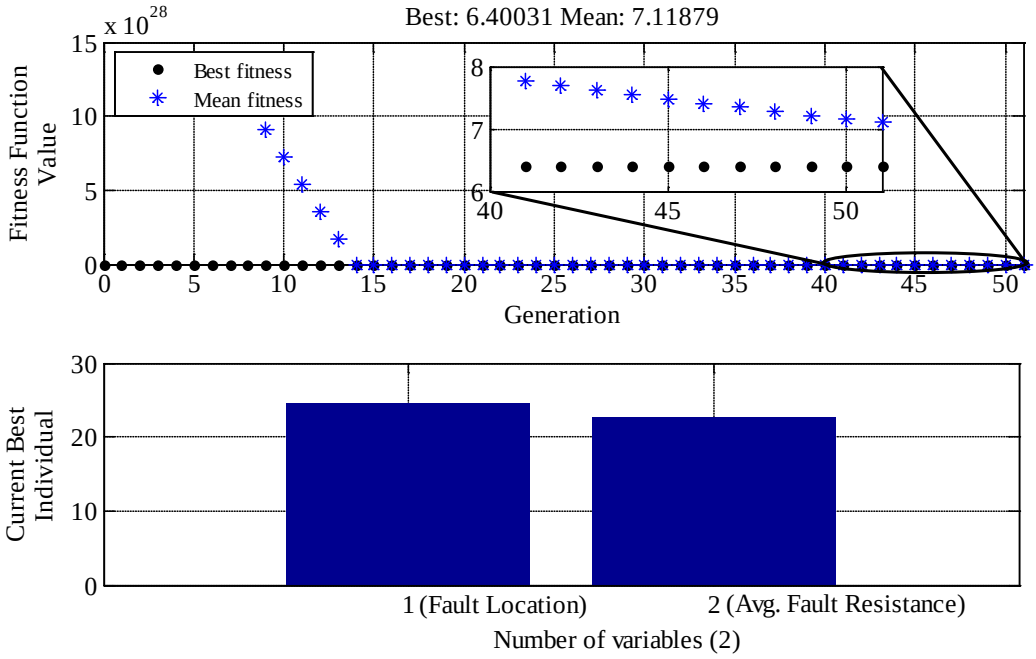

Fig. 4.15 GA results for turn-on condition

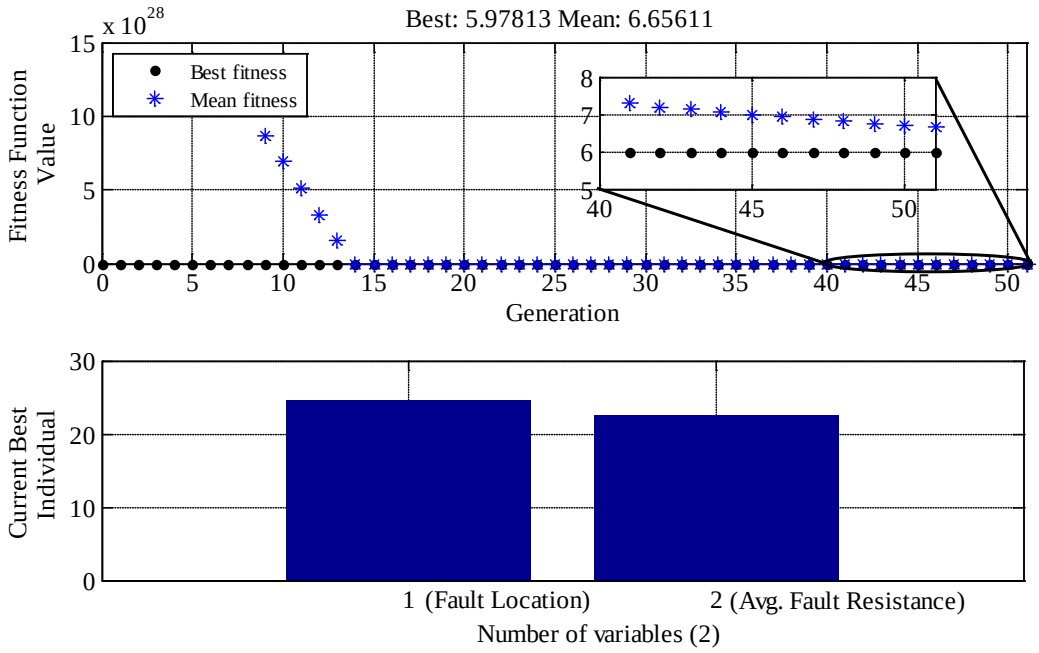

Fig. 4.16 GA results for turn-off condition

As mentioned in the previous chapter, GA does not minimize the fitness function under normal load circuit variations as shown in Fig. 4.15 and Fig. 4.16. In these cases, GA terminated the optimization procedure after 51 generations and produced d_1 as 24.6 meters, which is the upper boundary limit of the fault location.

From the above analysis, one thing is noticeable; the GA minimizes the fitness function only under fault conditions. This gives the additional potential to identify intermittent arc fault from normal aircraft PDS switching variations and/or load transients.

4.5 Summary

This chapter provides a simulation and experimental results on the proposed methods. The simulation model is developed in MARLAB/Simulink and formulas are written in MATLAB/mfile. The platform for experiments is prepared in the lab and is discussed in detail.

The model coefficients and wiring parameters are deviated from their normal values under fault conditions, which do satisfy the theory and mathematical modeling that was described in this thesis. Simulations were carried under three operating conditions such as turn-on of load circuit, normal and fault. Experiments were carried out under five operating conditions, turn-on of load circuit, normal, fault 1, fault 2 and turn-off of load circuit.

The proposed method has identified the intermittent arc fault based on deviations in model coefficients and wiring parameters, including not definable (N/D) wire resistance r and error e values. The genetic algorithm (GA) has estimated the intermittent arc location with an accuracy of +/- 0.5 meters on a 24.6 meter wire.

CHAPTER 5

CONCLUSIONS

5.1.Conclusion

This thesis addressed the effective and non-destructive diagnostic methods for intermittent arc fault detection and location, for solid state power controller (SSPC)-based aircraft power distribution system (PDS). The research was based on aircraft normal and faulty electrical load circuit modeling, model coefficients and wiring parameter estimation, and genetic algorithm.

The wiring-related problems and the importance of early wire fault detection are described in detail. The different aging factors, such as high and low temperatures, mechanical vibrations and stresses, environmental, electrical including over voltage and current, and physical are discussed in detail. It is investigated that chafe fault is one of the major origins for hazardous arc-related faults including intermittent arc. This persists over a long time period only if not detected and paves the road for serious faults. The phenomenon of dry line-to ground intermittent arc faults is investigated in the laboratory by mimicking the harsh aircraft environment. According to this study, it is noticed that the breached/damaged insulation can manifest as intermittent arc faults in unpredictable manners during mechanical vibrations or under mechanical stresses, always with short duration (about a few milliseconds) and low magnitudes.

Different existing methods for the aircraft wiring fault detection and location are discussed and analyzed in detail. Among these methods, it is identified that the sequence/spread spectrum time domain reflectometry (S/SSTDR) has received good attention for intermittent arc as well as hard faults detection and location because of its capacity to monitor the aircraft wires in real-time

manner. In conclusion, S/SSTDR and other methods such as acoustic sensors, power line communication (PLC) based carrier method and current sensors, etc., are not feasible for intermittent arc fault detection and location because they require dedicated sensors, transmitters, receivers, etc. These specialized pieces of hardware increase the cost, weight and maintenance expenses.

The main contributions of this thesis are described as follows:

- With the ABCD matrix (or transmission matrix) modeling method, the aircraft normal and faulty load modeling has been accomplished. In conclusion, the ABCD method can reduce the complexity of modeling the typical load circuit compared to the traditional differential equation approach by representing the wire segments, fault and load with cascaded two-port networks and has the advantage to model load circuit with more detailed structure when higher accuracy is required.
- From simulation and experimental studies, it has been noticed that intermittent arc faults in direct current (DC) PDS features the broadband frequency disturbance in voltage and current, and the voltage dips (or voltage sags). This phenomenon causes temporary deviations in model coefficients a_2, a_1, a_0, b_1, and b_0 and wire parameters r, l, c and g.
- A simple yet efficient method has been proposed to estimate the model coefficients and wiring parameters. In conclusion, based on temporary deviations of model coefficients and wiring parameters, intermittent arc fault detection is realized according to frequency domain information of circuit voltage and current signals on the source end.
- The fitness function has been formulated to estimate the fault-related parameters, such as intermittent arc location and average intermittent arc resistance.

- Genetic algorithm (GA) has been proposed to minimize the fitness function. In laboratory experiments and simulations, the proposed genetic algorithm has achieved intermittent arc location estimation with an accuracy of +/- 0.5 meters on 24.6 meter wire and 20 meter wire, respectively.
- Furthermore, the robustness of proposed methods has also been verified with the load turning-on and turning-off.

Future Work

This thesis presents the aircraft normal and faulty load circuit modeling, and its feasibility for intermittent arc fault detection and location. In addition, the following future work can be carried out to improve the potential of proposed methods:

- In this thesis, the proposed methods are analyzed with the resistive load. In addition, the proposed method can be verified with the different loads such as RL, RC, RLC and other aircraft loads, i.e., lights, motors, fans, etc. Accordingly, the methods described in chapter 3 need to modify and analyze. To do so, the complexity in computation will also increase.
- For the fitness function minimization, GA is used in this thesis. In addition, a new intelligent optimization method can also be introduced to estimate the fault-related parameters such as intermittent arc location and its average resistance; however, this means better accuracy and performance.
- Experiments using a DC power source have been conducted to verify the proposed methods. In addition, the proposed methods can also be analyzed with an alternating current (AC) power source.

REFERENCES

[1] J. A. Rosero, J. A. Ortega, E. Aldabas, and L. Romeral, “Moving towards a more electric aircraft,” IEEE Aerospace and Electronic Systems Magazine, vol. 22, no. 3, pp. 3-9, March 2007.

[2] K. R. Wheeler, D. A. Timucin, I. X. Twombly, K. F. Goebel, and P. F. Wysocki, Aging aircraft wiring fault detection survey, NASA Ames Research Center, Moffett Field, CA. [Online]. Available: http://ti.arc.nasa.gov/m/pub-archive/1342h/1342%20%28Wheeler%29.pdf

[3] C. Furse, and R. Haupt, “Down to the wire [aircraft wiring],” IEEE Spectrum, vol. 38, no. 2, pp. 34-39, Feb 2001.

[4] P. Smith, P. Kuhn, and C. Furse, “Intermittent fault location on live electrical wiring systems,” SAE International Journal of Aerospace, vol. 1, no. 1, pp. 1101-1106, April 2009.

[5] C. Furse, P. Smith, M. Safavi, and C. Lo, “Feasibility of spread spectrum sensors for location of arcs on live wires,” IEEE Sensors Journal, vol. 5, no. 6, pp. 1445-1450, Dec. 2005.

[6] M. W. Stavnes, and A. N. Hammoud, “Assessment of safety in space power wiring systems,” IEEE Aerospace and Electronics Magazine, vol. 9, no.1, Jan. 1994.

[7] C. Kim, “Detection and location of intermittent faults by monitoring carrier signal channel behavior of electrical interconnection system,” IEEE Electric Ship Technologies Symposium, pp.449-455, April 2009.

[8] G. Hickman, J. Gerardi, S. Field, and N. Kumbar, “An acoustic-based wiring diagnostic system for aircraft,” SAE Technical Paper, 2009.

[9] H.E. Orton, “Method for diagnosing degradation in aircraft wiring,” US Patent 6909977, Jun. 21, 2005.

[10] J. Kurek, P. R. Bernstein, M. Etheridge, G. Lasalle, R. McMahon, J Meiner, N. Turner, M. Walz, and C. Gomez, Aircraft wiring degradation study, Jan. 2008. [Online]. Available: http://www.tc.faa.gov/its/worldpac/techrpt/ar082.pdf

[11] C. Teal, and W. Larsen, “The phenomenology of wire, dielectrics and frequency [aircraft wiring],” The 21st Digital Avionics Systems Conference, vol. 2, pp. 12E6-1 – 12E6-9, Oct. 27-31, 2002.

[12] T. L. Johnson, and M. Ganesh, “Physics and measurement of early wire insulation chafing,” SAE International Journal of Aerospace, vol. 1, no. 1, pp. 1095-1100, April 2009.

[13] L. Griffiths, R. Parakh, C. Furse, and B. Baker, “The invisible fray: a critical analysis of the use of reflectometry for fray location,” IEEE Sensors Journal, vol. 6, no. 3, pp. 697-706, June 2006.

[14] C. Furse, Y.C. Chung, R. Dangol, M. Nielsen, G. Mabey, and R. Woodward, “Frequency-domain reflectometry for on-board testing of aging aircraft wiring," Electromagnetic Compatibility,” IEEE Transactions on Electromagnetic Compatibility, vol. 45, no. 2, pp. 306- 315, May 2003.

[15] C. Furse, Y. C Chung, L. Chet, and P. Pendayala, “ A critical comparison of reflectometry methods for location of wiring faults,” Smart Structures and Systems, vol. 2, no. 1, pp. 25-46, 2006. (Invited Paper)

[16] P. Smith, C. Furse, and J. Gunther, “Analysis of spread spectrum time domain reflectometry for wire fault location,” IEEE Sensors Journal, vol. 5, no. 6, pp. 1469-1478, Dec. 2005.

[17] S. Schuet, D. Timucin, and K. Wheeler, “A model-based probabilistic inversion framework for characterizing wire fault detection using TDR,” IEEE Transactions on Instrumentation and Measurement, vol. 60, no. 5, pp. 1654-1663, May 2011.

[18] P. Tsai, L. Chet, Y. C Chung, and C. Furse, “Mixed-signal reflectometer for location of faults on aging wiring,” IEEE Sensors Journal, vol. 5, no. 6, pp. 1479- 1482, Dec. 2005.

[19] S. Wu, C. Furse, and C. Lo, “Noncontact probes for wire fault location with reflectometry,” IEEE Sensors Journal, vol.6, no.6, pp.1716-1721, Dec. 2006.

[20] C. R. Sharma, C. Furse, and R. R. Harrison, “Low-power STDR CMOS sensor for locating faults in aging aircraft wiring,” IEEE Sensors Journal, vol. 7, no. 1, pp. 43-50, 2007.

[21] Z. Liu, R. J. Fuller, W. Yu, Y. Yang, and G. Liu, “Power line communication based aircraft power distribution system with real time wiring integrity monitoring capability,” US patent 7868621, Jan. 11, 2011.

[22] D. Izquierdo, A. Barrado, C. Raga, M. Sanz, and A. Lazaro, “Protection devices for aircraft electrical power distribution systems: state of the art,” IEEE Transactions on Aerospace and Electronic Systems, vol.47, no.3, pp. 1538-1550, July 2011.

[23] Y. C. Chung, N. N. Amarnath, and C. Furse, “Capacitance and Inductance Sensor Circuits for Detecting the Lengths of Open- and Short-Circuited Wires,” IEEE Transactions on Instrumentation and Measurement, , vol. 58, no. 8, pp. 2495-2502, Aug. 2009.

[24] J. B. Beck, and D. C. Nemir, “Arc fault detection through model reference estimation,” SAE Power Systems Conference, Session: Commercial Power Systems, New Orleans, LA, Nov. 2006.

[25] Y. Cao, and G. Liu, “Aircraft wiring fault evaluation based on modeling and parameter identification, International Conference on Mechatronics and Automation (ICMA), pp. 1969-1974, Aug. 7-10 2011.

[26] D. Lazarovich, I. Rusan, and D. knight, Arc fault detection for SSPC based electrical power distribution systems, US Patent 7177125, Feb. 13, 2007.

[27] K. Mussmacher and W.L. Froeb, “Controllers guard against arc faults,” Nov., 2004. [Online]. Available: http://powerelectronics.com/mag/411pet25.pdf

[28] Shang Chieh Wu, An iterative inverse method for transmission line fault location, PhD dissertation, Univ. Utah, Salt Lake City, UT, 2011.

[29] T. Gammon, and J. Matthews, “Instantaneous arcing-fault models for building system analysis,” IEEE transactions on Industry Applications, vol. 37, no. 1, pp. 197-203, Jan.-Feb. 2001.

[30] R. Alstine and G. Allan, Demonstration and validation of the excited dielectric test method to detect and locate defects in aircraft wiring systems, Jan. 2005. [Online]. Available: http://www.tc.faa.gov/its/worldpac/techrpt/ar04-43.pdf.

[31] A. Yaramasu, Y. Cao, G. Liu, and B. Wu, “Intermittent wiring fault detection and diagnosis for SSPC based aircraft power distribution system,” IEEE/ASME International Conference on Advanced Intelligent Mechatronics (AIM), pp. 1117-1122, July 11-14, 2012.

[32] R. F Ammerman, T. Gammon, P. K. Sen, J. P. Nelson, “DC-arc models and incident-energy calculations,” IEEE Transactions on Industry Applications, vol. 46, no. 5, pp.1810-1819, Sept.-Oct. 2010.

[33] X. Kang, J. Suonan, G. Song, and Z. Q. Bo, “Protection technique based on parameter identification — its principle and application,” IEEE Power and Energy Society General Meeting - Conversion and Delivery of Electrical Energy in the 21st Century, pp. 1-6, 20-24 July 2008.

[34] Gregory Levitin, The universal generating function in reliability analysis and optimization, Springer series in reliability engineering, 2005.

[35] E. J. Lundquist, and C. Furse, “Novel inverse methods for wire fault detection and diagnosis,” IEEE International Symposium on Antennas and Propagation (APSURSI), pp.2573-2576, July 2011.

[36] M. K. Smail, L. Pichon, M. Olivas, F. Auzanneau, and M. Lambert, “Detection of defects in wiring networks using time domain reflectometry,” IEEE Transactions on Magnetics, vol.46, no.8, pp. 2998-3001, Aug.2010.